Article

A Non-canonical Pathway with Potential for Safer Modulation of Transforming Growth Factor-β1 in Steroid-Resistant Airway Diseases

Meina Li, Christine R. Keenan, Guillermo Lopez-Campos, ..., Vinzenz Hofferek, Gavin E. Reid, Alastair G. Stewart

astew@unimelb.edu.au

HIGHLIGHTS

TGF-β1 extensively impairs GC activity

Phospho-cofilin1 is a key link in TGF-β1 signaling cascade subserving GC insensitivity

Phospho-cofilin1-activated phospholipase D (PLD) reduces GC activity

SMRT induction downstream of PLD mediates TGF-β1 impairment of GC activity

DATA AND SOFTWARE AVAILABILITY
GSE104908

Article

A Non-canonical Pathway with Potential for Safer Modulation of Transforming Growth Factor-β1 in Steroid-Resistant Airway Diseases

Meina Li,[1] Christine R. Keenan,[1] Guillermo Lopez-Campos,[2,3] Jonathan E. Mangum,[1] Qianyu Chen,[1] Danica Prodanovic,[1] Yuxiu C. Xia,[1] Shenna Y. Langenbach,[1] Trudi Harris,[1] Vinzenz Hofferek,[4,5] Gavin E. Reid,[5,6,7] and Alastair G. Stewart[1,8,9,*]

SUMMARY

Impaired therapeutic responses to anti-inflammatory glucocorticoids (GC) in chronic respiratory diseases are partly attributable to interleukins and transforming growth factor β1 (TGF-β1). However, previous efforts to prevent induction of GC insensitivity by targeting established canonical and non-canonical TGF-β1 pathways have been unsuccessful. Here we elucidate a TGF-β1 signaling pathway modulating GC activity that involves LIM domain kinase 2-mediated phosphorylation of cofilin1. Severe, steroid-resistant asthmatic airway epithelium showed increased levels of immunoreactive phospho-cofilin1. Phospho-cofilin1 was implicated in the activation of phospholipase D (PLD) to generate the effector(s) (lyso)phosphatidic acid, which mimics the TGF-β1-induced GC insensitivity. TGF-β1 induction of the nuclear hormone receptor corepressor, SMRT (NCOR2), was dependent on cofilin1 and PLD activities. Depletion of SMRT prevented GC insensitivity. This pathway for GC insensitivity offers several promising drug targets that potentially enable a safer approach to the modulation of TGF-β1 in chronic inflammatory diseases than is afforded by global TGF-β1 inhibition.

INTRODUCTION

Glucocorticoids (GCs) are widely used in the treatment of inflammatory and autoimmune diseases, such as asthma, chronic obstructive pulmonary disease (COPD), and rheumatoid arthritis (Rhen and Cidlowski, 2005). In most people with asthma, inflammation is well-controlled by inhaled GCs, whereas COPD-associated inflammation shows limited responsiveness to GCs. Moreover, approximately 10% of asthmatic patients remain symptomatic while using high doses of GCs (Chung et al., 2014). The pharmacodynamic manifestation of GC insensitivity includes a rightward shift in the concentration-response curve or a depression of the maximum response. Clinical GC insensitivity is defined as the presence of airway obstruction that is not relieved after 2 weeks of oral GC treatment, representing a reduction in the maximum GC response (Hew and Chung, 2010; Keenan et al., 2012).

GC activity in different cell types is dependent on the phenotype. Cell types not usually accorded a primary role in response to GCs, including epithelium, smooth muscle, and fibroblast, have well-documented capacity to add to the overall burden of inflammatory mediators (Keenan et al., 2012, 2015). Forming at the interface between the host and the environment, airway epithelium detects environmental stimuli and secretes a range of cytokines and chemokines that contribute to airway inflammation and airway structural changes in asthma (Lambrecht and Hammad, 2012) and are modulated by GC treatment. Thus the airway or lung epithelium is the site of deposition and significant actions of inhaled GCs. A corollary of the importance of the airway epithelium in asthma pathogenesis and GC activity is that in patients with GC insensitivity this cell type also has the potential to contribute to clinical GC resistance.

GC anti-inflammatory activity can be impaired by pro-inflammatory cytokines, resulting in the insensitivity to GCs in inflammatory diseases (Dejager et al., 2014). Inflammatory stimuli, including tumor necrosis factor alpha, interleukin-1β (IL-1β), IL-17A, or viral infection, contribute to GC insensitivity in epithelium (Rider et al., 2015; Webster Marketon and Corry, 2013; Zijlstra et al., 2012). However, the insensitivity induced by transforming growth factor β1 (TGF-β1) demands most attention because of its extraordinary capacity at picomolar concentrations to ablate GC anti-inflammatory activity in airway and lung epithelial cells (Keenan et al., 2014; Salem et al., 2012). Moreover, we have recently identified that viral infection of human

[1]Department of Pharmacology & Therapeutics, School of Biomedical Science, University of Melbourne, Parkville, VIC 3010, Australia

[2]Health and Biomedical Informatics Centre, Melbourne Medical School, University of Melbourne, Parkville, VIC 3010, Australia

[3]Centre for Experimental Medicine, Queen's University of Belfast, Belfast BT9 7BL, UK

[4]Max Plank Institute of Molecular Plant Physiology, Potsdam, Germany

[5]School of Chemistry, University of Melbourne, Parkville, VIC 3010, Australia

[6]Department of Biochemistry and Molecular Biology, University of Melbourne, Parkville, VIC 3010, Australia

[7]Bio21 Molecular Science and Biotechnology Institute. University of Melbourne, Parkville, VIC 3010, Australia

[8]ARC Centre for Personalised Therapeutics Technologies, Parkville, VIC, Australia

[9]Lead Contact

*Correspondence:
astew@unimelb.edu.au

https://doi.org/10.1016/j.isci.2019.01.023

bronchial epithelial cells impairs GC anti-inflammatory activity through the induction of TGF-β1 activity (Xia et al., 2017).

Increased activity of TGF-β1 in epithelium during the progression of inflammatory airway diseases is well documented (Honkova et al., 2014; Torrego et al., 2007). TGF-β1 is established as a key driver of remodeling in chronic respiratory diseases (Lachapelle et al., 2018). However, elevated levels of TGF-β1 in asthmatic patients are not suppressed by the use of GCs (Chakir et al., 2003). Global inhibition of TGF-β1 results in serious adverse effects including autoimmune colitis and cardiac valve defects (Anderton et al., 2011), precluding the acceptability of agents that inhibit receptor activation for non-oncological or life-threatening indications (Lachapelle et al., 2018). We have previously excluded roles for Smad4-dependent nuclear Smad signaling and the well-known non-canonical kinase pathways in the signaling of TGF-β1-induced GC insensitivity (Keenan et al., 2014). Moreover, TGF-β1-induced impairment is not associated with impaired GRα expression, nuclear location, or altered glucocorticoid receptor alpha (GRα) phosphorylation in BEAS-2B cell line (Keenan et al., 2014). Therefore a hitherto undescribed pathway mediating GC insensitivity needs further investigation. The elucidation of this signaling operating in parallel to, but independently of, established canonical and known non-canonical pathways offers the enticing prospect of selective, clinically tractable approaches to TGF-β1 modulation.

Here, we show by unbiased transcriptomic RNA sequencing (RNA-seq) analyses that the GC insensitivity induced by TGF-β1 is broad, rather than being restricted to genes regulated by transactivation. Moreover, we identify phospho-cofilin1 as an essential link in the signaling chain subserving TGF-β1-induced GC insensitivity using a combination of proteomic, pharmacological, and genetic approaches. The upstream signaling revealed a LIMK2 pathway leading to the phosphorylation of cofilin1. PLD, a known downstream effector of phospho-cofilin1 (Han et al., 2007), was implicated in the induction of the nuclear hormone corepressor, SMRT, the distal effector of GC insensitivity. We show here for the first time that the products of PLD-mediated membrane phospholipid remodeling, lysophosphatidic acid (LPA) and phosphatidic acid (PA), induce GC insensitivity.

RESULTS

TGF-β1 Has Extensive Modulatory Influence on GC Activity

To investigate the global impact of TGF-β1 on GC gene regulation, we conducted RNA-seq analyses of extracts of BEAS-2B cells (n = 3) incubated with TGF-β1 (40 pM), and then exposed to dexamethasone (Dex, 30 nM), using concentrations previously established as maximally effective (Keenan et al., 2014; Salem et al., 2012; Xia et al., 2017). Genes influenced by TGF-β1 alone by more than 2-fold and those with smaller but significant changes (applying a Benjamini and Hochberg [BH] false discovery rate [FDR] < 0.05) were filtered from the analyzed set to avoid the confounding influence of direct TGF-β1 gene regulation. Based on these criteria, 569 genes were differentially affected by Dex (BH FDR<0.05). Of the remaining 245 genes suppressed by Dex, 181 were less suppressed in the presence of TGF-β1. Similarly, of the 324 genes induced by Dex, 213 genes were induced to a lesser extent by the combination of TGF-β1 and Dex (Figure 1A). However, 40 genes downregulated by Dex showed greater downregulation following TGF-β1 conditioning and 91 genes showed greater upregulation than induced by Dex alone (Figure 1A). Thus, TGF-β1 predominantly limited the magnitude of GC induction and repression of gene expression. The TGF-β1/Dex interaction could be ascribed to a functional antagonism, whereby the effects of Dex are simply opposed by the effects of TGF-β1 driving expression in the opposite direction, rather than being related to the signal-transduction-based interaction that we propose. The exclusion of genes significantly affected by TGF-β1 mitigates against, but does not preclude, this possibility. Thus we examined adding the TGF-β1 "arithmetic effect" to the significant Dex effect and compared this result to the actual impact of prior TGF-β1 conditioning on the subsequent Dex response for each of the 569 analyzed Dex changes in gene expression. The absolute mean difference in the theoretically additive gene expression and the combined gene expression effect is $\log 2\ 0.55 \pm 0.02$ ($p < 10^{-15}$), indicating that the interaction is not explained by any residual (non-significant) effects of TGF-β1 opposing those of Dex (Table S1). The molecular mechanism of GC-regulated gene expression is mainly through transactivation via binding to positive glucocorticoid response element (pGRE) DNA-binding sequences and direct repression via binding to negative GRE (nGRE) DNA-binding sequences and transrepression. We further analyzed whether the TGF-β1 impairment is confined to subsets of genes containing pGRE or nGRE or to those genes bearing neither of the consensus GRE motifs in their promoter regions. We annotated our genes using DNA sequences derived from the literature (Surjit et al., 2011). Although the nGRE-containing genes were
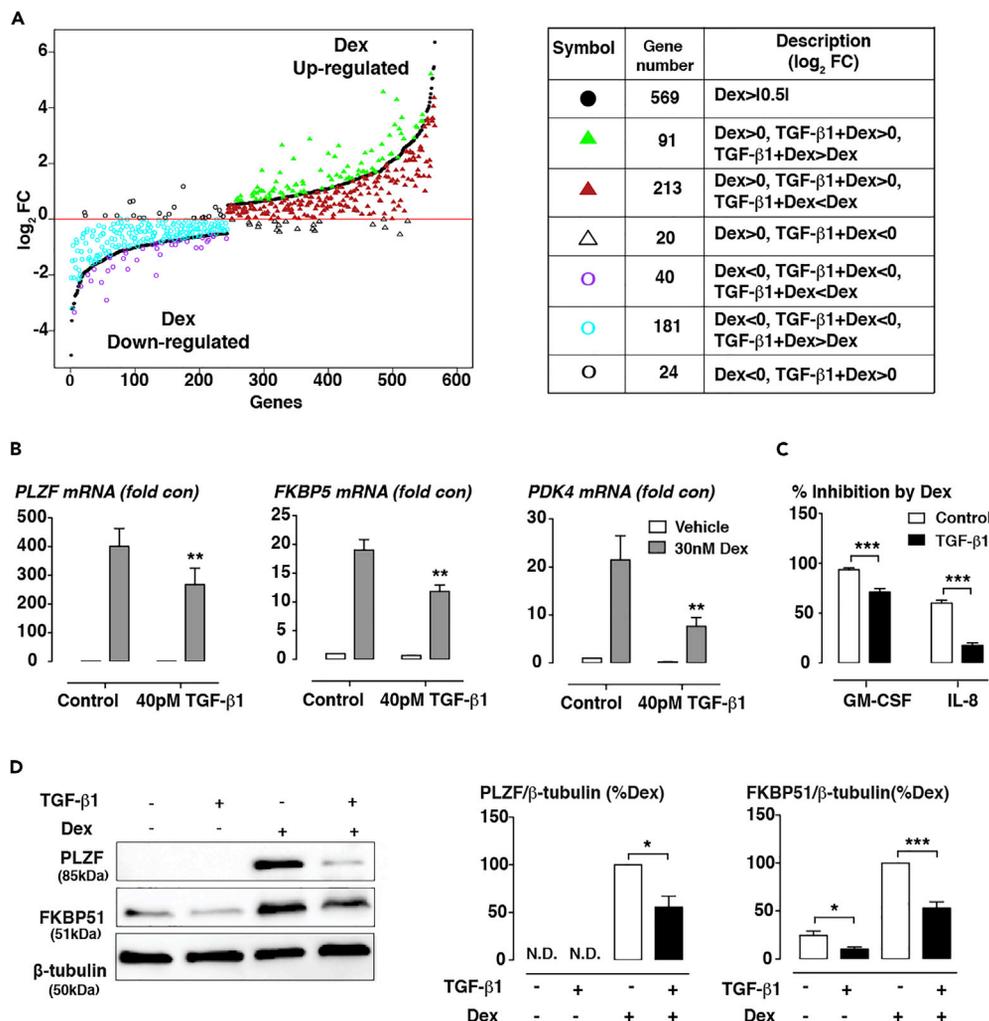
Figure 1. TGF-β1 Extensively Impairs GC Activity

(A) Analysis of transcriptomes of BEAS-2B cells incubated with Dex with or without TGF-β1 conditioning. Cells were pre-incubated with TGF-β1 (40 pM) for 24 h before stimulation with Dex (30 nM) or vehicle for 4 h. Data represent genes with a false discovery rate (FDR) <0.05 and not differentially affected by TGF-β1 alone ($-1 < \log_2$ FC < 1 or FDR > 0.05). Numbers of genes with specific patterns of GC-regulated expression are presented in the accompanying table together with graphical symbols.

(B) Quantitative real-time PCR (qRT-PCR) analysis of selected GC-inducible genes.

(C) Effects of TGF-β1 on pro-inflammatory cytokine levels regulated by GC. A549 cells were incubated with TGF-β1 (40 pM) for 12 h and incubated with Dex (10 nM) 30 min before incubation with IL-1α (1 ng/mL) for another 16 h. Levels of GM-CSF and IL-8 were measured by ELISA.

(D) Effects of TGF-β1 on the expression of GC-regulated proteins. BEAS-2B cells were incubated with TGF-β1 (40 pM) for 24 h and incubated with Dex (30 nM) for another 24 h.

Representative western blots are shown and aggregated data are presented as mean ± SEM. (A) n = 3, (B) n = 5–6, (C) n = 5, and (D) n = 6. N.D., not detectable. FC, fold control. Two-way ANOVA is used for (B); two-tailed Student's t test is used for (C, D). *p < 0.05, **p < 0.01, ***p < 0.001. (See also Tables S1, S2, and S3).

under-represented in the set of genes that showed TGF-β1 impairment of Dex-induced gene expression, the impairment effect is observed with genes that express nGRE, pGRE, both, or neither (Table S2). Moreover, "FunRich" gene set enrichment analyses suggested that TGF-β1-modulated Dex-influenced genes across different biological pathways and processes (Table S3).

We investigated the underlying mechanism with a focus on the specific TGF-β1 impairment of GC-induced genes documented as effectors of GC anti-inflammatory activity and regulation of cytokine production.

GC-induced mRNA encoding promyelocytic leukemia zinc finger (PLZF), FK506-binding protein 51 (FKBP5), and pyruvate dehydrogenase kinase 4 (PDK4) were suppressed by TGF-β1 (Figure 1B). GC induction of increased levels of the PLZF and FKBP5 proteins was also reduced by TGF-β1 (Figure 1D). TGF-β1 impairment of GC transrepressional mechanisms has been characterized in the A549 cell line (Salem et al., 2012), so we used the A549 cell line to investigate TGF-β1 impairment of GC transrepression. TGF-β1 attenuated the maximum inhibitory effect of Dex on IL-1α-induced IL-8 and granulocyte-macrophage colony-stimulating factor (GM-CSF) production in the A549 cell line (Figure 1C). The impact of these effects can be appreciated when considering that the levels of GM-CSF increase approximately 10-fold from 12 ± 5 pg/mL in the presence of IL1α/Dex to 106 ± 24 pg/mL, in cells additionally conditioned by TGF-β1. Thus our characterization indicates that TGF-β1 impairs GC-regulated gene expression changes in airway epithelial cells via mechanisms that transcend discrete transcriptional influences of GC, such as those dependent on nGRE, pGRE, or transcription factor repression.

Proteomic Analysis Reveals Phospho-cofilin1 as the Primary Candidate Mediator in TGF-β1-Induced GC Insensitivity

We had excluded roles for Smad4 and a wide range of non-canonical kinase signaling pathways in the TGF-β1 modulation of steroid signaling, suggesting the involvement of a new pathway (Keenan et al., 2014). Candidate signaling proteins were assessed by an operational proteomic approach afforded by 2-dimensional differential in gel electrophoresis (2D-DIGE). We prioritized candidate protein expression changes by exploiting an unexpected difference in the activity of the different TGF-β gene products, whereby both TGF-β1 and TGF-β3 impaired GRE activity, but TGF-β2 was inactive in both BEAS-2B and A549 cells (Figure S1A). The bioactivity of TGF-β2 was validated not only by its induction of Smad7 (Figure S1B) but also by the induction of seven changes in 2D-DIGE protein spots (Figure 2A). The 2D-DIGE experiment in BEAS-2B cells treated with each of TGF-β1–3 revealed that of the 748 ± 35 (n = 5) protein spots detected, three spots were differentially expressed in extracts from TGF-β1- or TGF-β3-incubated cells, but not in those incubated with TGF-β2 (Figure 2A). Moreover, these changes in protein expression were insensitive to inhibition by a combination of mitogen-activated protein kinase (MAPK) and phosphatidylinositol 3-kinase (PI3K) pathway inhibitors that had been previously established to be individually ineffective on the TGF-β1-induced GC insensitivity (Keenan et al., 2014; Salem et al., 2012) and are now confirmed to be ineffective when used in combination (Figures S1C and S1D). These three spots were therefore prioritized for identification by picking and then subjected to tryptic digest before analysis by liquid chromatography-tandem mass spectrometry. The data were then analyzed by Mascot to identify the candidate proteins (listed in Table S4).

Phospho-cofilin1 was prioritized over the two other candidates because over-expression of cofilin1 had been reported to inhibit GR activity (Ruegg et al., 2004), and the cofilin1 levels of lymphocytes from steroid-insensitive asthmatic patients had been found to be inversely correlated with the ability of GC to suppress cytokine release (Vasavda et al., 2006). TGF-β1 and TGF-β3, but not TGF-β2, increased the phosphorylation of cofilin1 through MAPK-independent pathways (Figures 2B and S1E). Moreover, the elevation of phospho-cofilin1 levels by TGF-β1 was suppressed by 1 μM SB431542 (TβRI kinase inhibitor) (Figure S2A). Upon TGF-β1 treatment, phospho-cofilin1 protein levels increased, whereas Smad3 levels decreased (Figure S2B), consistent with the suggestion that TGF-β1 increased phospho-cofilin1 levels via a Smad3-independent, non-canonical kinase-dependent signaling pathway. However, further experiments are required to make this conclusion, given that the Smad3-targeted small interfering RNA (siRNA) did not further reduce the low Smad3 levels observed in the presence of TGF-β1 (Figure S2B). Incubation with cofilin1-targeted siRNA, which reduced cofilin1 protein levels to less than 20%, markedly diminished the level of TGF-β1-induced phospho-cofilin1 (Figure 2C). Cofilin1 siRNA completely prevented TGF-β1 inhibition of PLZF and FKBP5 gene expression (Figure 2D). The percentage of TGF-β1 suppression of Dex-induced ENaCα (epithelial sodium channel α) and PDK4 mRNA expression was reduced by cofilin1-targeting siRNA from $53\% \pm 5\%$ to $37\% \pm 3\%$ and from $54\% \pm 8\%$ to $38\% \pm 5\%$, respectively. The relevance of phospho-cofilin1 was underlined by its elevated expression in the airway epithelium in biopsies from patients with severe, steroid-resistant asthma (see Table S5 for demographic data) compared with non-asthmatic subjects or those with mild-moderate asthma (Figure 2E).

TGF-β1-Induced Suppression of GC Activity Is due to the Activation of LIMK2

Cofilin1 phosphorylation is effected principally by the LIM domain kinase (LIMK). We therefore examined the effect of the putative upstream kinase LIMK using the small-molecule inhibitor, LIMKi3 (Scott et al., 2010). Cofilin1 phosphorylation was concentration-dependently reduced by LIMKi3 (1–10 μM). LIMKi3
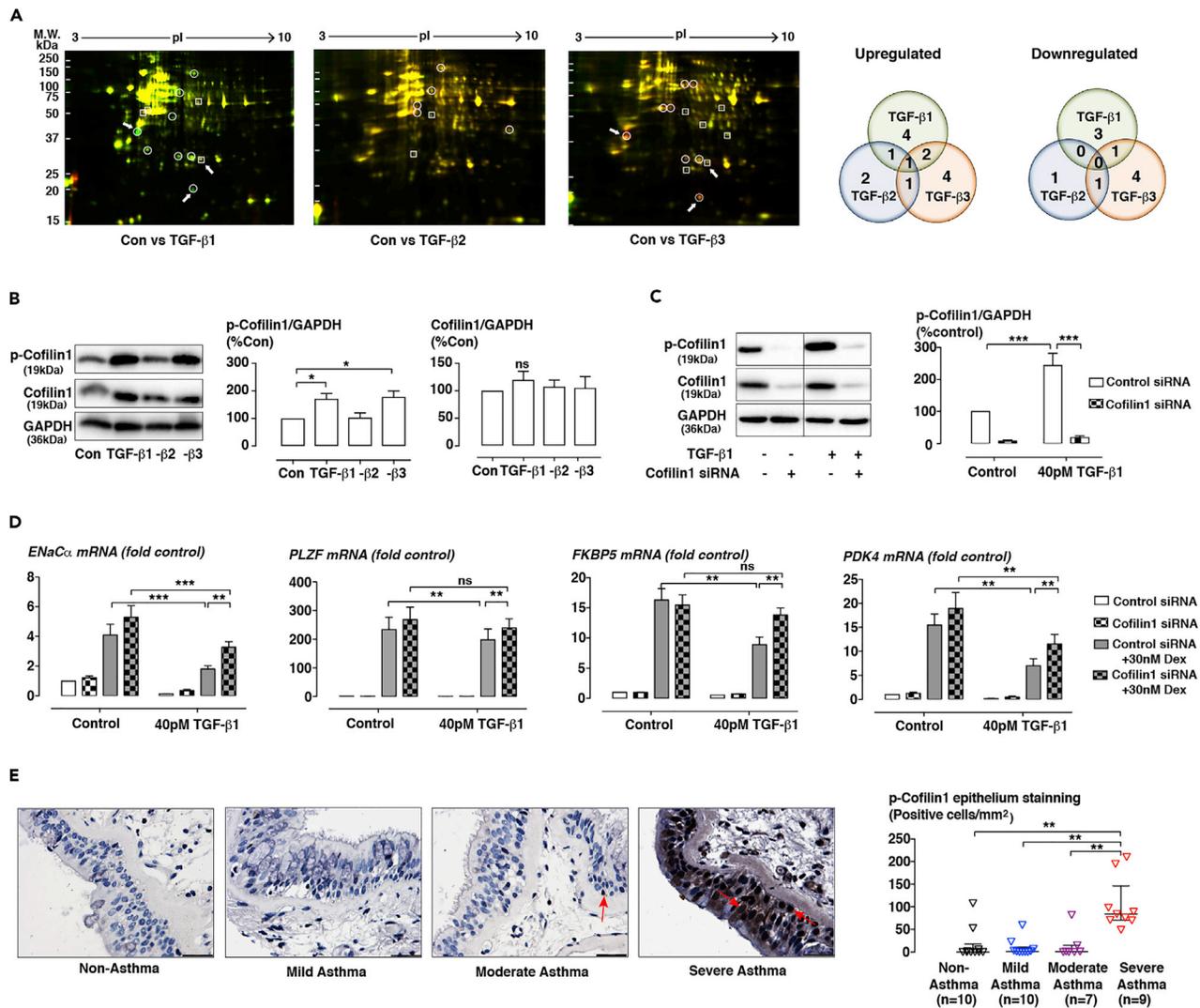
Figure 2. Proteomic Analyses Prioritize Phospho-cofilin1 As a Mediator in TGF-β1-Induced GC Insensitivity

(A) The 2D-DIGE comparative analysis between control and TGF-β isoforms. BEAS-2B cells were incubated with TGF-β isoforms (40 pM each) for 24 h, and lysates were subjected to 2D-DIGE. Overlay of Cy3 and Cy5 derived from a representative gel, highlighting differentially expressed protein spots: round for up-regulation; square for down-regulation. CyDye minimal labeling as follows: Control-Cy5 versus TGF-β1-Cy3; Control-Cy3 versus TGF-β2-Cy5; Control-Cy3 versus TGF-β3-Cy5. Venn diagram shows distribution of differentially expressed protein spots with TGF-β isoforms.

(B) Independent validation of TGF-β induction of phospho-cofilin1 by western blot.

(C) Western blot validation of successful knockdown of cofilin1 by cofilin1-targeted siRNA. (D) Effects of genetic ablation of cofilin1 on TGF-β1 impairment of GC-inducible gene expression. BEAS-2B cells were transfected with negative control or cofilin1-targeted siRNA, incubated with TGF-β1 (40pM) for 24h, and then incubated with Dex (30nM) for another 4h.

(E) Phospho-cofilin1 immunoreactivity in airway biopsies from subjects with increasing asthma severity scale bar, 30 μm.

Results are presented as mean ± SEM or mean with interquartile range. (A) n = 3–5, (B) n = 5, (C and D) n = 4–5, (E) n = 7–10. ns, not significant. Two-way ANOVA is used for (C, D); two-tailed paired Student's t test is used for (A, B); non-parametric Kruskal-Wallis is used for (E). *p < 0.05, **p < 0.01, ***p < 0.001. (See also Figures S1 and S2 and Table S4).

(10 μM) completely prevented TGF-β1-induced elevation of phospho-cofilin1 levels (Figure 3A), but had no effect on Plasminogen activator inhibitor-1 (PAI-1) mRNA expression (Figure 3B), a Smad3-and Smad4-dependent TGF-β1 effect (Keenan et al., 2014). LIMKi3 prevented TGF-β1 suppression of GC induction of GILZ, PLZF, FKBP5, and PDK4 gene expression (Figure 3B) and partially restored ENaCα gene expression (Figure 3B) and GRE activity (Figures S3A and S3B). Reduction of LIMK2 expression by approximately 50% using siRNA attenuated TGF-β1 impairment of GC-regulated PLZF and FKBP5 expression (Figure 3C), whereas a 70% reduction of LIMK1 had no effect (Figure S3C). The differential influence of LIMK1 and
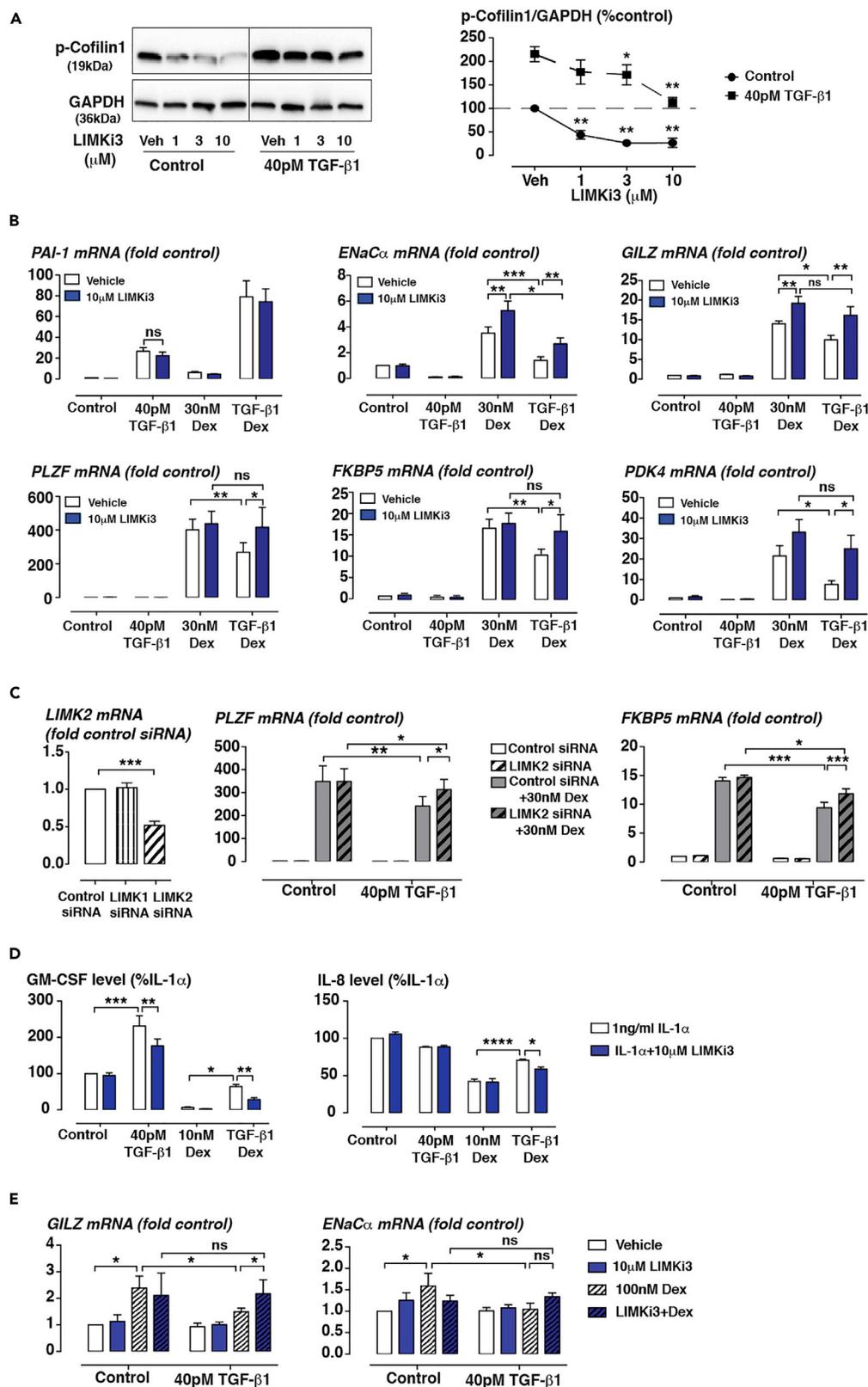
Figure 3. TGF-β1-Induced Impairment of GC Activity Is Dependent on LIM Kinase 2 Activity

(A) Pharmacological inhibition of LIMK inhibits TGF-β1-induced increase in phospho-cofilin1 levels. BEAS-2B cells were incubated with LIMKi3 (1–10 μM) for 30 min before incubation with TGF-β1 (40 pM) for 24 h.

(B) Smad-dependent PAI-1 and GC-inducible gene expression targets were determined by qRT-PCR in BEAS-2B cells incubated with LIMKi3 (10 μM) for 30 min before TGF-β1 (40 pM) for 24 h followed by incubation with Dex (30 nM) for 4 h.

(C) BEAS-2B cells transfected with negative control or LIMK2-targeted siRNA were incubated with TGF-β1 (40 pM) for 24 h, followed by incubation with Dex (30 nM) for 4 h before mRNA measurement.

(D) Levels of GM-CSF and IL-8 were measured by ELISA and expressed as a percentage of the IL-1α response. A549 cells were incubated with LIMKi3 (10 μM) for 30 min before TGF-β1 (40 pM) for 12 h and incubated with Dex (10 nM) 30 min before incubation with IL-1α (1 ng/mL) for another 16 h.

(E) Effects of pharmacological inhibition of LIMK on TGF-β1 impairment of GC activity in human bronchial epithelial cells differentiated for 28 days at air-liquid interface (ALI). Cells were incubated with LIMKi3 (10 μM) 30 min before incubation with TGF-β1 (40 pM) for 24 h, then incubated with Dex (100 nM) or vehicle control for 4 h.

Data are presented as mean ± SEM from n = 4 individual donors. (A–D) n = 5–6 (E) = 4. ns, not significant. Two-way ANOVA is used for (A–D); two-tailed paired Student's t test is used for (E). *p < 0.05, **p < 0.01, ***p < 0.001, ****p < 0.0001. (See also Figure S3).

LIMK2 on the TGF-β1-impaired GC activity is consistent with accumulating evidence demonstrating the potential association of LIMK2 level, but not LIMK1, with asthma severity in inflammatory cells (Aoki et al., 2009; Bigler et al., 2017; Persson et al., 2015).

In A549 cells, IL-1α-induced elevation of GM-CSF level was completely prevented by Dex. TGF-β1 enhanced IL-1α-induced increases in GM-CSF levels and compromised the Dex suppression of GM-CSF levels. Inhibition of LIMK using LIMKi3 (10 μM) restored much of the activity of Dex in suppressing both GM-CSF and IL-8 levels (Figure 3D).

We have previously established the TGF-β1 modulation of GC in air-liquid interface (ALI) differentiated primary human epithelial organotypic cultures (Keenan et al., 2014). This organotypic culture setting engenders a differentiated cell population expressing functional activity, such as beating cilia and mucous production, and an intact epithelial barrier. In ALI cultures, TGF-β1 inhibition of Dex-induced GILZ and ENaCα expression was prevented by the inhibition of LIMK (Figure 3E).

There is a well-established connection between the TGF-β1 receptor and RhoA/B and GTP-bound Cdc42 activation (Kardassis et al., 2009). Moreover, LIMK activation is widely thought to result from phosphorylation by ROCK or Cdc42/PAK (Lee-Hoeflich et al., 2004; Sumi et al., 2000). These TGF-β1-activated pathways have been documented in a signaling chain in Swiss 3T3 fibroblasts (Vardouli et al., 2005), but are not yet evidenced in an epithelial cell phenotype. Hence, we investigated the effects of blocking ROCK (10 μM Y27632), Cdc42 (5 μM ML141), or both using well-validated inhibitors at concentrations that have been previously reported by other groups to effectively inhibit the respective enzymatic activities (Hong et al., 2013; Sumi et al., 2000). Neither the ROCK inhibitor or the Cdc42 inhibitor alone nor their combination was able to even partially mimic the effect of inhibiting LIMK (Figures 4A and S4A).

Cofilin1 phosphorylation at serine 3 by LIM domain kinase switches off the actin filament severing activity of cofilin1 (Vardouli et al., 2005). However, neither LIMKi3 (10 μM) nor the inhibitor of Cdc42 ML141 (5 μM) affected the TGF-β1-induced re-distribution of actin between F and G forms. The ROCK inhibitor Y27632 (10 μM) prevented TGF-β1-induced increases in F-actin levels (Figure 4B), as did the F-actin-disrupting agent, cytochalasin B (Figure S4B), but neither Y27632 nor cytochalasin B restored GC-inducible gene expression (Figures 4A and S4C). These findings dissociate actin cytoskeletal changes induced by TGF-β1 from impaired GC responses.

TGF-β1 Impairment of GC Activity Is due to Phospho-cofilin1-Dependent Phospholipase D Activation

Although cofilin1 is widely regarded as the active form of the protein, phospho-cofilin1 has also been reported to activate phospholipase D1 (PLD1) (Han et al., 2007). We therefore examined the possible involvement of PLD in TGF-β1 signaling of GC insensitivity, using the selective inhibitors VU01550699 (7.5 μM) or FIPI (10 μM), at concentrations based on previous studies (Kang et al., 2013; Su et al., 2009) and as further validated in our initial experiments. Incubation of BEAS-2B cells with VU01550699 (7.5 μM) prevented TGF-β1 suppression of Dex-induced expression of GILZ, ENaCα, and FKBP5 and substantially enhanced Dex-induced GILZ mRNA expression (Figure 5A). Use of FIPI (10 μM) further confirmed the involvement of the PLD in TGF-β1 suppression of GC-regulated gene expression (Figure 5B). Moreover, both
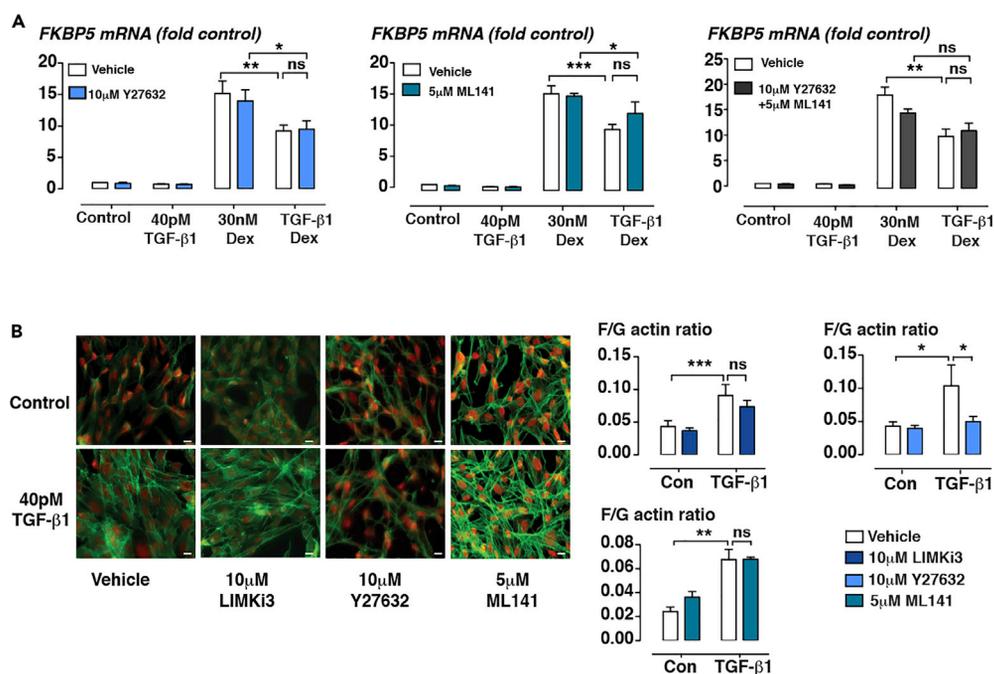
Figure 4. TGF-β1-Induced Impairment of GC Activity Is Not Due to the Activity of ROCK/Cdc42 or TGF-β1-Induced Actin Reorganization

(A) BEAS-2B cells were incubated with the ROCK inhibitor Y27632 (10 μM) or the Cdc42 inhibitor ML141 (5 μM) for 30 min before TGF-β1 (40 pM, 24 h incubation) followed by Dex (30 nM) incubation for 4 h before mRNA measurement.

(B) Fluorescence imaging of F-actin (green) and G-actin (red) in BEAS-2B cells incubated with LIMKi3 (10 μM), Y27632 (10 μM), and ML141 (5 μM) 30 min before TGF-β1 (40 pM) for 24 h; scale bar, 50 μm.

Data are presented as mean ± SEM. (A) n = 3–6, (B) n = 3–6. Two-way ANOVA is used throughout. *p < 0.05, **p < 0.01, ***p < 0.001. ns, not significant. (See also Figure S4).

VU01550699 and FIPI reduced TGF-β1 impairment of Dex-induced GRE activity (Figure S5A). PLD was further implicated by the restoration of GC responsiveness through the use of PLD1/2-targeted siRNA, with combined knockdown of PLD1 and PLD2 attenuating the TGF-β1 inhibition of Dex-induced FKBP5 and PLZF mRNA expression (Figure 5C). Individual PLD1 and PLD2 knockdown each attenuated the inhibitory effects of TGF-β1 on GILZ and PLZF mRNA expression (Figure S5B). The TGF-β1 impairment of Dex suppression of pro-inflammatory cytokines GM-CSF and IL-8 levels was prevented by the inhibition of PLD by VU01550699 (7.5 μM) (Figure 5D), as was the TGF-β1-induced inhibition of GILZ and ENaCα expression in the ALI cultures (Figure 5E). These data strongly supported a role for PLD in the signaling downstream of phospho-cofilin1 to mediate TGF-β1 impairment of GC activity.

Activation of PLD increases the hydrolysis of phosphatidylcholine (PC) to choline and the second messenger lipid PA, which may be further metabolized to LPA and diacylglycerol (Csaki et al., 2013). Exogenous PLD products, PA and LPA, mimicked the effect of TGF-β1 in repressing the Dex-induced GRE activity (Figure S5C) and in decreasing GRE-regulated genes (Figures 5F and 5G), without cytotoxicity (Figure S5D). The mimicry of TGF-β1 by exogenous (lyso)phosphatidic acid could suggest that these PC metabolites were being mobilized as autocrine mediators of TGF-β1. This possibility was examined by the transfer of TGF-β1-conditioned supernatant to TGF-β1-naive BEAS-2B cells. BEAS-2B cells were incubated with TGF-β1 (40 pM) for 6 or 24 h to generate conditioned medium. Before transfer to serum-starved BEAS-2B cells, the ALK5 inhibitor SB431542 (10 μM) was added to the medium to block ALK5 signaling induced by the transferred TGF-β1. The conditioned medium did not contain a transferable GC suppressive factor (Figures S6A and S6B), leading us to conclude that the (lyso)phosphatidic acid induced by TGF-β1 acts within the intracellular compartment. Phospholipid remodeling could allow LPA access to LPA receptors, whereas blockade of LPA receptors (1–3) using Ki16425 (10 μM) (Ohta et al., 2003) had no effect on the impairment of GC-induced gene expression caused by either TGF-β1 or (lyso)phosphatidic acid (Figure S6C).
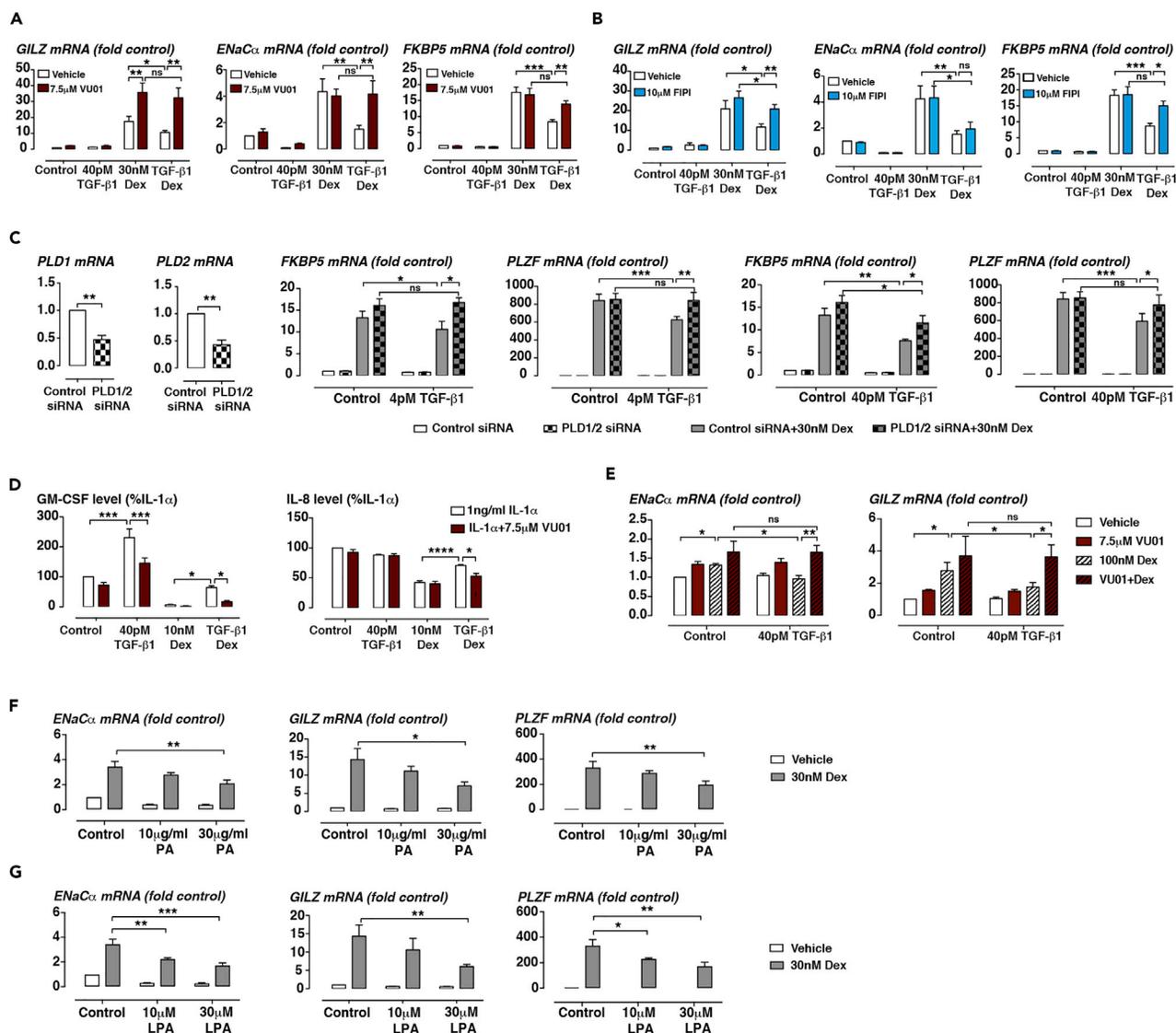
Figure 5. Inhibition of Phospholipase D (PLD) Prevents TGF-β1 Induction of GC Insensitivity

(A and B) Effects of PLD inhibitors (A) VU0155069 (VU01, 7.5 μM) or (B) FIPI (10 μM) on TGF-β1-induced suppression of GC-inducible gene expression was investigated.

(C) Effects of genetic depletion of PLD1/2 on TGF-β1-suppressed GC activity was investigated by qRT-PCR.

(D) Levels of GM-CSF and IL-8 were measured by ELISA and expressed as a percentage of the IL-1α response. A549 cells were incubated with VU0155069 (7.5 μM) for 30 min before TGF-β1 (40 pM) for 12 h and incubated with Dex (10 nM) 30 min before incubation with IL-1α (1 ng/mL) for another 16 h.

(E) Effects of pharmacological inhibition of PLD on TGF-β1 impairment of GC activity in human bronchial epithelial cells differentiated for 28 days at air-liquid interface (ALI).

(F and G) Effects of exogenous PA and LPA on Dex-inducible gene expression. BEAS-2B cells were exposed to (F) PA (10 or 30 μg/mL) or (G) LPA (10 or 30 μM) for 24 h, before incubation with Dex (30 nM) for 4 h.

Data are presented as mean ± SEM. (A–D) n = 4–5, (E–G) n = 4. ns, not significant. Two-way ANOVA is used for (A–D; F–G); two-tailed paired Student's t test is used for (E). *p < 0.05, **p < 0.01, ***p < 0.001, ****p < 0.0001. (See also Figure S5).

SMRT Induction Downstream of Phospho-cofilin1/PLD Mediates TGF-β1-Induced Repression of GR Target Gene Expression

The repressive activities of TGF-β1 and PA on peroxisome proliferator-activated receptor (PPAR) have been previously ascribed to stabilization of the PPAR interaction with the corepressor SMRT in macrophages and fibroblasts (Stockert et al., 2011; Tsukahara et al., 2010). We therefore analyzed whether TGF-β1 influences SMRT in BEAS-2B cells. TGF-β1 significantly increased SMRT levels, an effect that was dependent on the
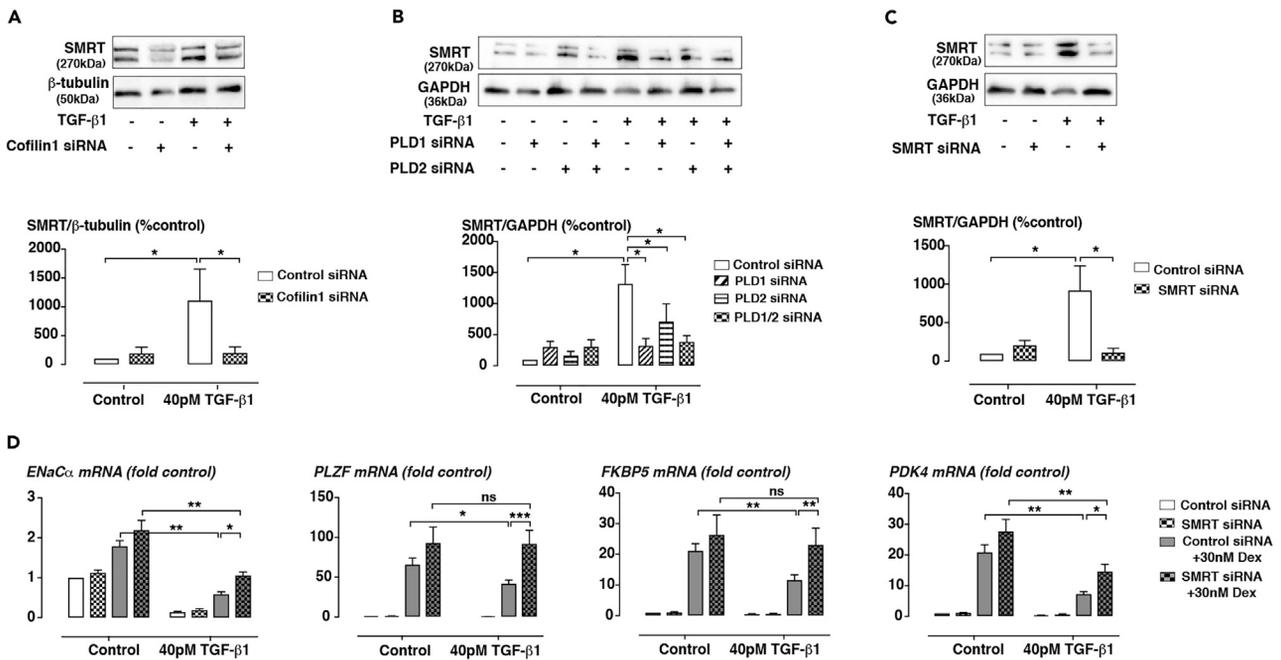
Figure 6. SMRT Induction Downstream of Phospho-cofilin1/PLD Activity Plays a Role in the TGF-β1-Induced Repression of GR Target Genes

(A and B) Effects of genetic deletion of (A) cofilin1 and (B) PLD1/2 on SMRT expression. Cell lysates were the same as those used in Figures 2D and 5C.

(C) Validation of successful knockdown of SMRT-targeted siRNA in BEAS-2B cells. (D) Effects of genetic ablation of SMRT on GC-inducible gene expression. BEAS-2B cells transfected with negative control or SMRT-targeted siRNA, were incubated with TGF-β1 (40pM) for 24h, and then incubated with Dex (30nM) for another 4h before mRNA measurement.

Data are presented as mean ± SEM. (A–D) n = 5. ns, not significant. Two-way ANOVA is used for (A–D). *p < 0.05, **p < 0.01, ***p < 0.001. (See also Figure S7).

action of cofilin1 and PLD (Figures 6A and 6B). SMRT-targeted siRNA prevented the TGF-β1 induction of SMRT protein levels (Figure 6C), preventing TGF-β1 suppression of PLZF and FKBP5 mRNA, and attenuating suppression of ENaCα (percentage inhibition reduced from 67% ± 4% to 50% ± 5%) and PDK4 (percentage inhibition reduced from 65% ± 3% to 47% ± 4%) mRNA expression, respectively (Figures 6D, S7A, and S7B). Moreover, TGF-β1, PA, and LPA each completely prevented the transcriptional regulation of CYP27A1 (encoding cytochrome P450 family 27 subfamily A member 1) by the PPARγ agonist, rosiglitazone (Figure S8), consistent with a role for intracellular PA in mediating TGF-β1 inhibition of the nuclear hormone receptors, GR and PPARγ.

DISCUSSION

We identified a broad modulatory impact of TGF-β1 on GC activity, showing reduced maximal responses of both GC-induced and GC-repressed genes. A TGF-β1 signaling pathway was elucidated comprising LIMK2-mediated phosphorylation of cofilin1 that requires PLD1 and PLD2 enzyme activity and induction of the nuclear hormone corepressor SMRT (Figure 7). The increased expression of phospho-cofilin1 in the airway epithelium of severe, steroid-resistant asthmatic patients further supported the relevance of our findings, which we believe will facilitate drug discovery efforts focused on safely blocking the contribution of TGF-β1 to chronic inflammatory diseases (Lachapelle et al., 2018).

The relative importance of transactivation and transrepression to the anti-inflammatory activity of GC remains controversial (Keenan et al., 2015). GR dimer-dependent transactivation is increasingly regarded as essential for certain of the anti-inflammatory activities of GR (Vandevyver et al., 2013). As TGF-β1 suppressed GC-sensitive genes associated with pGRE, nGRE, transrepression, or other mechanisms of regulation with similar frequencies, the exogenous TGF-β1 effect is not limited in scope to a specific GC gene regulatory mechanism. We selected a panel of GRE-dependent GC-responsive genes, including GILZ, ENaCα, PLZF, PDK4, FKBP5, as well as the cytokines, GM-CSF and IL-8, to assess the impact of TGF-β1 on GC sensitivity. This selection was based on their importance in inflammation, as described briefly below,
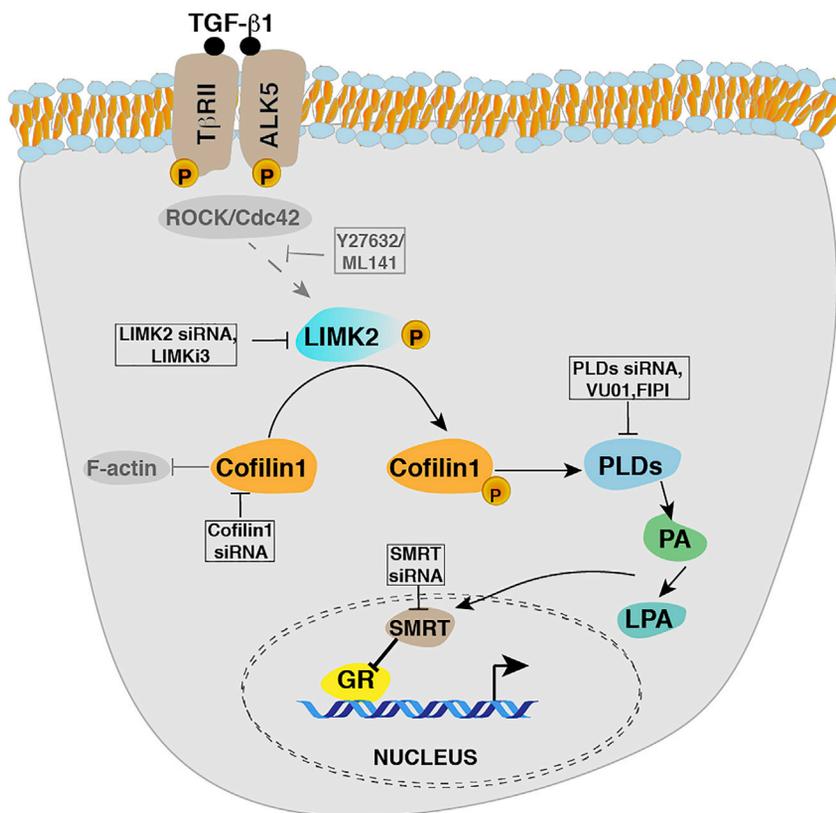
Figure 7. LIMK2-Mediated Cofilin1 Phosphorylation Signals TGF-β1-Induced GC Insensitivity
Phospho-cofilin1 is implicated as a key link in the chain of signalling behavior of TGF-β1-induced GC insensitivity. The activation of LIMK2 appears to be independent of known upstream regulators ROCK or Cdc42. Phospho-cofilin1-activated PLD mediates SMRT induction, which limits GR target gene regulation. The interventions including small-molecule inhibitors and siRNA are summarized in boxes.

and having comparative data from prior studies (Keenan et al., 2014; Salem et al., 2012; Xia et al., 2017). GILZ mediates some of the anti-inflammatory effects of Dex in epithelial cells (Eddleston et al., 2007). Impaired epithelium sodium channel expression results in excess fluid and pulmonary edema (Kerem et al., 1999). FKBP5 is not only a biomarker of GC responsiveness but also is implicated in modulating the nuclear translocation and transcriptional activity of nuclear factor-κB (Erlejman et al., 2014). PLZF is a GC-inducible transcription factor that arrests cell cycle by inducing the expression of CDK inhibitors (Naito et al., 2015). PDK4 inactivates the pyruvate dehydrogenase complex (PDC), which catalyzes the conversion of pyruvate to acetyl-CoA. PDC metabolite flux is involved in the immunometabolic reprogramming of macrophages, a process that allows cellular defense mechanisms to accommodate the different micro-environments encountered in inflamed tissues (O'Neill and Pearce, 2016). Imparied GC induction of GILZ, ENaCα, FKBP5, PLZF, and PDK4 could amplify inflammation in the airway wall in asthma.

TGF-β1 impaired GC regulatory effects on the pro-inflammatory cytokines, IL-8 and GM-CSF. IL-8, a power-ful chemoattractant and activator of neutrophils, is detected at increased levels in severe asthma (Shannon et al., 2008). Neutrophils are generally considered to be less directly sensitive to GC treatment. In GC-resis-tant asthma, inhibition of IL-8 release by GC is impaired (Nair et al., 2015; Wang et al., 2016). GM-CSF facilitates robust eosinophilic inflammation, long-lasting antigen-specific Th2 inflammation, mucous pro-duction, and airway hyperresponsiveness (Llop-Guevara et al., 2014). The compromised GC regulation of these inflammogens in epithelia conditioned by TGF-β1 is likely to contribute to the severity and limit the therapeutic responsiveness of chronic inflammation to GCs.

Global inhibition of TGF-β1 or ALK5 activity is known to increase the risk of autoimmune disorders and heart valve lesions (Anderton et al., 2011). Therefore further understanding of the TGF-β1 signaling cascades that

interfere with GC activity may identify targets downstream of the receptors for selective restoration of GC responses, which avoid the detrimental effect of global TGF-β1 inhibition (Lachapelle et al., 2018). We used a hypothesis-free proteomic approach to examine the signaling of GC resistance by TGF-β1 because hypothesis-driven approaches, including the use of a wide panel of kinase inhibitors and effective Smad4 inhibition (Keenan et al., 2014; Salem et al., 2012), had been exhausted without success. Three candidate signaling proteins were prioritized by (1) inclusion of protein changes common to the active TGF-β forms, TGF-β1 and TGF-β3; (2) exclusion of changes induced by TGF-β2, which did not induce GC impairment; and (3) exclusion of changes that were prevented by the combination of MAPK and PI3K-targeting small-molecule inhibitors that failed to block TGF-β1 impairment of GC responses. Phospho-cofilin1 was further prioritized based on studies implicating cofilin1 in steroid sensitivity (Ruegg et al., 2004; Vasavda et al., 2006).

As one of the main activities of cofilin1 is actin severing, our attention turned to the possibility that TGF-β1 impairment of GC activity could be secondary to changes in the actin cytoskeleton, and possibly to influences on cellular mechanics (Krishnan et al., 2016). However, pharmacological inhibitors of LIMK and ROCK/Cdc42 showed differential effects on TGF-β1-induced phosphorylated-cofilin1, GC insensitivity, and actin polymerization. The ROCK inhibitor and cytochalasin B prevented TGF-β1 induction of F-actin levels without restoring GC activity, whereas the LIMK inhibitor prevented cofilin1 phosphorylation and restored GC activity, without effect on TGF-β1-induced F-actin. These observations do not support a role for actin cytoskeletal assembly in the regulation of GC sensitivity.

Although phospho-cofilin1 had been widely considered to be inactive, it was subsequently convincingly demonstrated to be an activator of PLD1 (Han et al., 2007, 2011). Aberrant PLD activity has been identified in chronic inflammatory autoimmune disorders and in allergic asthma (Choi et al., 2015; Kang et al., 2013). Moreover, TGF-β1 increases PLD activity and increases the levels of PA and PA-related metabolites in epithelial cell lines (Zhou et al., 2000). We sought to establish whether there is a link between PLD and the TGF-β1 suppression of GC activity. TGF-β1 suppression of GC activity in epithelial cells was prevented by reducing the activity of PLD, consistent with a pivotal role for phospho-cofilin1-activated PLD in TGF-β1 impairment of GC activity (Figure 7). Importantly, exogenous PA and LPA mimicked the effects of TGF-β1 on a panel of Dex-inducible genes and GRE activity. This observation linking PA or LPA and GC sensitivity has implications beyond TGF-β1 to a broader relationship between PLD products and GC sensitivity. The levels of polyunsaturated LPA in human bronchoalveolar lavage (BAL) fluid increase 3-fold after segmental allergen challenge (to ~1.5 μM) (Georas et al., 2007). When accounting for ~100-fold dilution of airway surface fluid by the instilled lavage fluid, the epithelium may be exposed to LPA *in situ* of over 100 μM, which exceeds the concentrations of exogenous LPA and PA required to mimic GC resistance. LPA present in biological fluids, such as plasma and BAL, is thought to initiate effects in airway inflammation and remodeling by activation of cell surface G-protein coupled LPA$_{1-7}$ receptors (Zhao and Natarajan, 2013), leading to the question of whether TGF-β1 mobilized LPA to exert intra- or extracellular effects. However, a series of careful supernatant transfer experiments indicated that the TGF-β1 impairment of GC activity was not accompanied by the release of transferable activity in the conditioned medium. Moreover, blockade of LPA receptors had no effect on the impairment of GC activity caused by either TGF-β1 or exogenous PA or LPA. Therefore extracellular activation of LPA receptors is less likely to account for the TGF-β1 effect than intracellular mobilization and action of PLD products.

Both PA and LPA are reported to bind to certain nuclear hormone receptors, including PPARγ (McIntyre et al., 2003). PA has been shown to inhibit PPARγ transactivation with high potency and high specificity, by stabilizing the interaction of PPARγ with the corepressor SMRT (Tsukahara et al., 2010). Moreover, PA has a biphasic influence on epidermal growth factor receptor (EGFR) expression, whereby lower concentrations of PA enable and higher concentrations impede PPARα/LXRα binding to the EGFR promoter (Henkels et al., 2016). We have now shown that the corepressor SMRT is a transcriptional target of TGF-β1 through a chain of signaling linking CK1δ/ε to phospho-cofilin1-activated PLD. The siRNA-mediated inhibition of SMRT leads to a strong derepression of TGF-β1-targeted GR gene expression, suggesting that SMRT signals GC resistance downstream of the activated PLD.

In summary, we establish that TGF-β1 potently induces insensitivity to GC activity. Pharmacological and genetic approaches implicated a chain of signaling through LIMK2/phospho-cofilin1/PLD, liberating PA and LPA to induce GC insensitivity through the induction of SMRT. Our findings identify new drug targets to modulate TGF-β1 that may be amenable to safe modulation by avoiding interference in essential growth

and immunoregulatory TGF-β1 activities that are mediated by canonical and well-established non-canonical pathways operating upstream or independently of this pathway.

Limitations of the Study

We have provided compelling evidence that SMRT links TGF-β1 and GC activity, acting through a chain of signaling involving LIMK2 to phospho-cofilin1-activated PLD to induce GC insensitivity. However, the detailed mechanism underlying ALK5-mediated increases in the level of phospho-cofilin1 and PLD-mediated increases in the level of SMRT remain unsolved. We aim to address the translational significance of our findings in future studies designed to better understand the physiological functions of the identified novel non-canonical TGF-β1 signaling pathway in steroid-resistant airway diseases.

METHODS

All methods can be found in the accompanying Transparent Methods supplemental file

DATA AND SOFTWARE AVAILABILITY

The accession number for the RNA-seq data reported in this paper is GEO Database: GSE104908

SUPPLEMENTAL INFORMATION

Supplemental Information includes Transparent Methods, eight figures, and five tables and can be found with this article online at https://doi.org/10.1016/j.isci.2019.01.023.

AUTHOR CONTRIBUTIONS

A.G.S. and M.L. conceived the study and designed the experiments. M.L., C.R.K., D.P., Q.C., V.H., and G.E.R. performed experiments and analyzed data. G.L.-C. and J.E.M. helped with bioinformatic analysis. Y.C.X., S.Y.L., and T.H., assisted with experiment design. M.L. and A.G.S. wrote the manuscript. All authors edited and approved submission of the manuscript.

DECLARATION OF INTERESTS

The authors declare no competing interests.

REFERENCES

Anderton, M.J., Mellor, H.R., Bell, A., Sadler, C., Pass, M., Powell, S., Steele, S.J., Roberts, R.R., and Heier, A. (2011). Induction of heart valve lesions by small-molecule ALK5 inhibitors. Toxicol. Pathol. 39, 916–924.

Aoki, T., Matsumoto, Y., Hirata, K., Ochiai, K., Okada, M., Ichikawa, K., Shibasaki, M., Arinami, T., Sumazaki, R., and Noguchi, E. (2009). Expression profiling of genes related to asthma exacerbations. Clin. Exp. Allergy 39, 213–221.

Bigler, J., Boedigheimer, M., Schofield, J.P.R., Skipp, P.J., Corfield, J., Rowe, A., Sousa, A.R., Timour, M., Twehues, L., Hu, X., et al. (2017). A severe asthma disease signature from gene expression profiling of peripheral blood from U-BIOPRED cohorts. Am. J. Respir. Crit. Care Med. 195, 1311–1320.

Chakir, J., Shannon, J., Molet, S., Fukakusa, M., Elias, J., Laviolette, M., Boulet, L.-P., and Hamid, Q. (2003). Airway remodeling-associated mediators in moderate to severe asthma: Effect of steroids on TGF-β, IL-11, IL-17, and type I and type III collagen expression. J. Allergy Clin. Immunol. 111, 1293–1298.

Choi, H.J., Park, S.Y., Cho, J.H., Park, J.W., Sohn, J.H., Kim, Y.J., Oh, J.W., and Han, J.S. (2015). The TLR4-associated phospholipase D1 activation is crucial for Der f 2-induced IL-13 production. Allergy 70, 1569–1579.

Chung, K.F., Wenzel, S.E., Brozek, J.L., Bush, A., Castro, M., Sterk, P.J., Adcock, I.M., Bateman, E.D., Bel, E.H., Bleecker, E.R., et al. (2014). International ERS/ATS guidelines on definition, evaluation and treatment of severe asthma. Eur. Respir. J. 43, 343–373.

Csaki, L.S., Dwyer, J.R., Fong, L.G., Tontonoz, P., Young, S.G., and Reue, K. (2013). Lipins, lipinopathies, and the modulation of cellular lipid storage and signaling. Prog. Lipid Res. 52, 305–316.

Dejager, L., Vandevyver, S., Petta, I., and Libert, C. (2014). Dominance of the strongest: inflammatory cytokines versus glucocorticoids. Cytokine Growth Factor Rev. 25, 21–33.

Eddleston, J., Herschbach, J., Wagelie-Steffen, A.L., Christiansen, S.C., and Zuraw, B.L. (2007). The anti-inflammatory effect of glucocorticoids is mediated by glucocorticoid-induced leucine zipper in epithelial cells. J. Allergy Clin. Immunol. 119, 115–122.

Erlejman, A.G., De Leo, S.A., Mazaira, G.I., Molinari, A.M., Camisay, M.F., Fontana, V., Cox, M.B., Piwien-Pilipuk, G., and Galigniana, M.D. (2014). NF-kappaB transcriptional activity is modulated by FK506-binding proteins FKBP51 and FKBP52: a role for peptidyl-prolyl isomerase activity. J. Biol. Chem. 289, 26263–26276.

Georas, S.N., Berdyshev, E., Hubbard, W., Gorshkova, I.A., Usatyuk, P.V., Saatian, B., Myers, A.C., Williams, M.A., Xiao, H.Q., Liu, M., et al. (2007). Lysophosphatidic acid is detectable in human bronchoalveolar lavage fluids at baseline and increased after segmental allergen challenge. Clin. Exp. Allergy 37, 311–322.

Han, L., Stope, M.B., de Jesus, M.L., Oude Weernink, P.A., Urban, M., Wieland, T., Rosskopf, D., Mizuno, K., Jakobs, K.H., and Schmidt, M. (2007). Direct stimulation of receptor-controlled phospholipase D1 by phospho-cofilin. EMBO J. 26, 4189–4202.

Han, X., Yu, R., Ji, L., Zhen, D., Tao, S., Li, S., Sun, Y., Huang, L., Feng, Z., Li, X., et al. (2011). InlB-mediated Listeria monocytogenes internalization requires a balanced phospholipase D activity maintained through phospho-cofilin. Mol. Microbiol. 81, 860–880.

Henkels, K.M., Miller, T.E., Ganesan, R., Wilkins, B.A., Fite, K., and Gomez-Cambronero, J. (2016). A Phosphatidic Acid (PA) conveyor system of continuous intracellular transport from cell membrane to nucleus maintains EGF receptor homeostasis. Oncotarget 7, 47002–47017.

Hew, M., and Chung, K.F. (2010). Corticosteroid insensitivity in severe asthma: significance, mechanisms and aetiology. Intern. Med. J. 40, 323–334.

Hong, L., Kenney, S.R., Phillips, G.K., Simpson, D., Schroeder, C.E., Noth, J., Romero, E., Swanson, S., Waller, A., Strouse, J.J., et al. (2013). Characterization of a Cdc42 protein inhibitor and its use as a molecular probe. J. Biol. Chem. 288, 8531–8543.

Honkova, L., Uhlik, J., Berankova, K., Svobodova, T., and Pohunek, P. (2014). Epithelial basement membrane thickening is related to TGF-Beta 1 expression in children with chronic respiratory diseases. Pediatr. Allergy Immunol. 25, 593–599.

Kang, D.W., Park, M.K., Oh, H.J., Lee, D.G., Park, S.H., Choi, K.Y., Cho, M.L., and Min do, S. (2013). Phospholipase D1 has a pivotal role in interleukin-1beta-driven chronic autoimmune arthritis through regulation of NF-kappaB, hypoxia-inducible factor 1alpha, and FoxO3a. Mol. Cell. Biol. 33, 2760–2772.

Kardassis, D., Murphy, C., Fotsis, T., Moustakas, A., and Stournaras, C. (2009). Control of transforming growth factor beta signal transduction by small GTPases. FEBS J. 276, 2947–2965.

Keenan, C.R., Mok, J.S., Harris, T., Xia, Y., Salem, S., and Stewart, A.G. (2014). Bronchial epithelial cells are rendered insensitive to glucocorticoid transactivation by transforming growth factor-beta1. Respir. Res. 15, 55.

Keenan, C.R., Radojicic, D., Li, M., Radwan, A., and Stewart, A.G. (2015). Heterogeneity in mechanisms influencing glucocorticoid sensitivity: the need for a systems biology approach to treatment of glucocorticoid-resistant inflammation. Pharmacol. Ther. 150, 81–93.

Keenan, C.R., Salem, S., Fietz, E.R., Gualano, R.C., and Stewart, A.G. (2012). Glucocorticoid-resistant asthma and novel anti-inflammatory drugs. Drug Discov. Today 17, 1031–1038.

Kerem, E., Bistritzer, T., Hanukoglu, A., Hofmann, T., Zhou, Z., Bennett, W., MacLaughlin, E., Barker, P., Nash, M., Quittell, L., et al. (1999). Pulmonary epithelial sodium-channel dysfunction and excess airway liquid in pseudohypoaldosteronism. N. Engl. J. Med. 341, 156–162.

Krishnan, R., Park, J.A., Seow, C.Y., Lee, P.V., and Stewart, A.G. (2016). Cellular biomechanics in drug screening and evaluation: mechanopharmacology. Trends Pharmacol. Sci. 37, 87–100.

Lachapelle, P., Li, M., Douglass, J., and Stewart, A. (2018). Safer approaches to therapeutic modulation of TGF-beta signaling for respiratory disease. Pharmacol. Ther. 187, 98–113.

Lambrecht, B.N., and Hammad, H. (2012). The airway epithelium in asthma. Nat. Med. 18, 684–692.

Lee-Hoeflich, S.T., Causing, C.G., Podkowa, M., Zhao, X., Wrana, J.L., and Attisano, L. (2004). Activation of LIMK1 by binding to the BMP receptor, BMPRII, regulates BMP-dependent dendritogenesis. EMBO J. 23, 4792–4801.

Llop-Guevara, A., Chu, D.K., Walker, T.D., Goncharova, S., Fattouh, R., Silver, J.S., Moore, C.L., Xie, J.L., O'Byrne, P.M., Coyle, A.J., et al. (2014). A GM-CSF/IL-33 pathway facilitates allergic airway responses to sub-threshold house dust mite exposure. PLoS One 9, e88714.

McIntyre, T.M., Pontsler, A.V., Silva, A.R., St Hilaire, A., Xu, Y., Hinshaw, J.C., Zimmerman, G.A., Hama, K., Aoki, J., Arai, H., et al. (2003). Identification of an intracellular receptor for lysophosphatidic acid (LPA): LPA is a transcellular PPARgamma agonist. Proc. Natl. Acad. Sci. U S A 100, 131–136.

Nair, P., Aziz-Ur-Rehman, A., and Radford, K. (2015). Therapeutic implications of 'neutrophilic asthma'. Curr. Opin. Pulm. Med. 21, 33–38.

Naito, M., Vongsa, S., Tsukune, N., Ohashi, A., and Takahashi, T. (2015). Promyelocytic leukemia zinc finger mediates glucocorticoid-induced cell cycle arrest in the chondroprogenitor cell line ATDC5. Mol. Cell. Endocrinol. 417, 114–123.

O'Neill, L.A., and Pearce, E.J. (2016). Immunometabolism governs dendritic cell and macrophage function. J. Exp. Med. 213, 15–23.

Ohta, H., Sato, K., Murata, N., Damirin, A., Malchinkhuu, E., Kon, J., Kimura, T., Tobo, M., Yamazaki, Y., Watanabe, T., et al. (2003). Ki16425, a subtype-selective antagonist for EDG-family lysophosphatidic acid receptors. Mol. Pharmacol. 64, 994–1005.

Persson, H., Kwon, A.T., Ramilowski, J.A., Silberberg, G., Soderhall, C., Orsmark-Pietras, C., Nordlund, B., Konradsen, J.R., de Hoon, M.J., Melen, E., et al. (2015). Transcriptome analysis of controlled and therapy-resistant childhood asthma reveals distinct gene expression profiles. J. Allergy Clin. Immunol. 136, 638–648.

Rhen, T., and Cidlowski, J.A. (2005). Antiinflammatory action of glucocorticoids—new mechanisms for old drugs. N. Engl. J. Med. 353, 1711–1723.

Rider, C.F., Shah, S., Miller-Larsson, A., Giembycz, M.A., and Newton, R. (2015). Cytokine-induced loss of glucocorticoid function: effect of kinase inhibitors, long-acting beta(2)-adrenoceptor [corrected] agonist and glucocorticoid receptor ligands. PLoS One 10, e0116773.

Ruegg, J., Holsboer, F., Turck, C., and Rein, T. (2004). Cofilin 1 is revealed as an inhibitor of glucocorticoid receptor by analysis of hormone-resistant cells. Mol. Cell. Biol. 24, 9371–9382.

Salem, S., Harris, T., Mok, J.S., Li, M.Y., Keenan, C.R., Schuliga, M.J., and Stewart, A.G. (2012). Transforming growth factor-beta impairs glucocorticoid activity in the A549 lung adenocarcinoma cell line. Br. J. Pharmacol. 166, 2036–2048.

Scott, R.W., Hooper, S., Crighton, D., Li, A., Konig, I., Munro, J., Trivier, E., Wickman, G., Morin, P., Croft, D.R., et al. (2010). LIM kinases are required for invasive path generation by tumor and tumor-associated stromal cells. J. Cell Biol. 191, 169–185.

Shannon, J., Ernst, P., Yamauchi, Y., Olivenstein, R., Lemiere, C., Foley, S., Cicora, L., Ludwig, M., Hamid, Q., and Martin, J.G. (2008). Differences in airway cytokine profile in severe asthma compared to moderate asthma. Chest 133, 420–426.

Stockert, J., Adhikary, T., Kaddatz, K., Finkernagel, F., Meissner, W., Muller-Brusselbach, S., and Muller, R. (2011). Reverse crosstalk of TGFbeta and PPARbeta/delta signaling identified by transcriptional profiling. Nucleic Acids Res. 39, 119–131.

Su, W., Yeku, O., Olepu, S., Genna, A., Park, J.S., Ren, H., Du, G., Gelb, M.H., Morris, A.J., and Frohman, M.A. (2009). 5-Fluoro-2-indolyl des-chlorohalopemide (FIPI), a phospholipase D pharmacological inhibitor that alters cell

spreading and inhibits chemotaxis. Mol. Pharmacol. 75, 437–446.

Sumi, T., Matsumoto, K., and Nakamura, T. (2000). Specific activation of LIM kinase 2 via phosphorylation of threonine 505 by ROCK, a rho-dependent protein kinase. J. Biol. Chem. 276, 670–676.

Surjit, M., Ganti, K.P., Mukherji, A., Ye, T., Hua, G., Metzger, D., Li, M., and Chambon, P. (2011). Widespread negative response elements mediate direct repression by agonist-liganded glucocorticoid receptor. Cell 145, 224–241.

Torrego, A., Hew, M., Oates, T., Sukkar, M., and Fan Chung, K. (2007). Expression and activation of TGF-beta isoforms in acute allergen-induced remodelling in asthma. Thorax 62, 307–313.

Tsukahara, T., Tsukahara, R., Fujiwara, Y., Yue, J., Cheng, Y., Guo, H., Bolen, A., Zhang, C., Balazs, L., Re, F., et al. (2010). Phospholipase D2-dependent inhibition of the nuclear hormone receptor PPARgamma by cyclic phosphatidic acid. Mol. Cell 39, 421–432.

Vandevyver, S., Dejager, L., Tuckermann, J., and Libert, C. (2013). New insights into the anti-inflammatory mechanisms of glucocorticoids: an emerging role for glucocorticoid-receptor-mediated transactivation. Endocrinology 154, 993–1007.

Vardouli, L., Moustakas, A., and Stournaras, C. (2005). LIM-kinase 2 and cofilin phosphorylation mediate actin cytoskeleton reorganization induced by transforming growth factor-beta. J. Biol. Chem. 280, 11448–11457.

Vasavda, N., Eichholtz, T., Takahashi, A., Affleck, K., Matthews, J.G., Barnes, P.J., and Adcock, I.M. (2006). Expression of nonmuscle cofilin-1 and steroid responsiveness in severe asthma. J. Allergy Clin. Immunol. 118, 1090–1096.

Wang, M., Gao, P., Wu, X., Chen, Y., Feng, Y., Yang, Q., Xu, Y., Zhao, J., and Xie, J. (2016). Impaired anti-inflammatory action of glucocorticoid in neutrophil from patients with steroid-resistant asthma. Respir. Res. 17, 153.

Webster Marketon, J.I., and Corry, J. (2013). Poly I: C and respiratory syncytial virus (RSV) inhibit glucocorticoid receptor (GR)-mediated transactivation in lung epithelial, but not monocytic, cell lines. Virus Res. 176, 303–306.

Xia, Y.C., Radwan, A., Keenan, C.R., Langenbach, S.Y., Li, M., Radojicic, D., Londrigan, S.L., Gualano, R.C., and Stewart, A.G. (2017). Glucocorticoid insensitivity in virally infected airway epithelial cells is dependent on transforming growth factor-beta activity. PLoS Pathog. 13, e1006138.

Zhao, Y., and Natarajan, V. (2013). Lysophosphatidic acid (LPA) and its receptors: role in airway inflammation and remodeling. Biochim. Biophys. Acta 1831, 86–92.

Zhou, B.H., Chen, J.S., Chai, M.Q., Zhao, S., Liang, J., Chen, H.H., and Song, J.G. (2000). Activation of phospholipase D activity in transforming growth factor-beta-induced cell growth inhibition. Cell Res. 10, 139–149.

Zijlstra, G.J., Ten Hacken, N.H., Hoffmann, R.F., van Oosterhout, A.J., and Heijink, I.H. (2012). Interleukin-17A induces glucocorticoid insensitivity in human bronchial epithelial cells. Eur. Respir. J. 39, 439–445.

Supplemental Information

A Non-canonical Pathway with Potential

for Safer Modulation of Transforming Growth Factor-β1

in Steroid-Resistant Airway Diseases

Meina Li, Christine R. Keenan, Guillermo Lopez-Campos, Jonathan E. Mangum, Qianyu Chen, Danica Prodanovic, Yuxiu C. Xia, Shenna Y. Langenbach, Trudi Harris, Vinzenz Hofferek, Gavin E. Reid, and Alastair G. Stewart
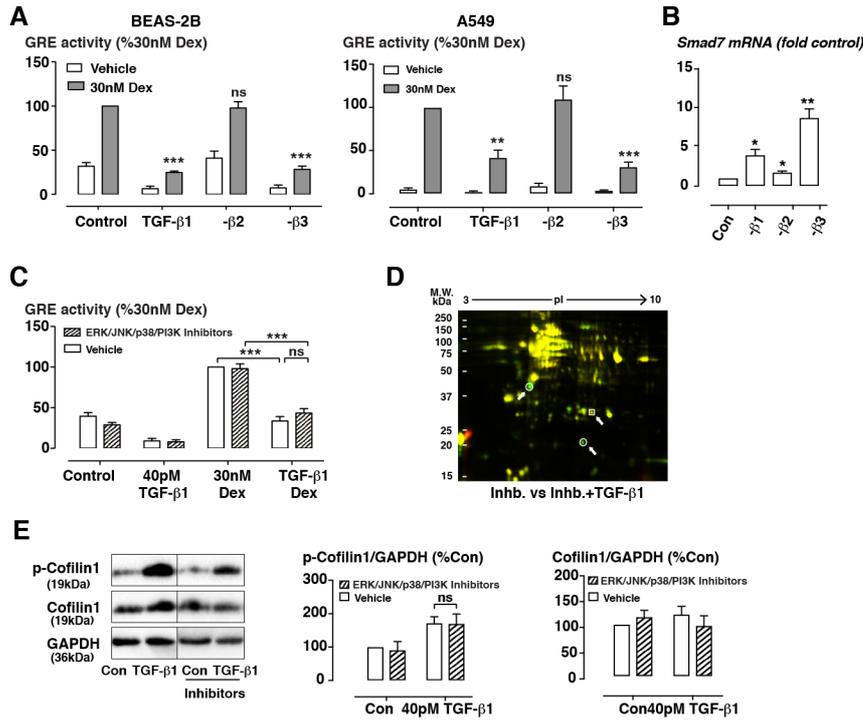
Figure S1. Strategies for narrowing the candidate pool, **related to Figure 2.** (A) Effects of TGF-β1-3 on Dex-induced GRE activity in BEAS-2B and A549 cells transiently transfected with GRE-SEAP reporter constructs and incubated with TGF-β1, TGF-β2 or TGF-β3 (40pM each). (B) Serum-starved BEAS-2B cells were incubated with TGF-β1, TGF-β2 or TGF-β3 (40pM each) for 28h before mRNA measurement. (C) BEAS-2B cells transiently transfected with GRE-SEAP reporter construct were incubated with the combination of inhibitors of p38^{MAPK} (1μM SB202190), ERK1/2 (1μM U0126), JNK (1μM SP600125), PI3K (10μM LY294002) for 30 min prior and during exposure to TGF-β1 (40pM) for 24h, followed by Dex (30nM) for another 24h. (D) The 2D-DIGE comparative analysis between control and TGF-β1 in the presence of multiple kinase inhibitors. Inhibitors (Inhb.)-Cy5 vs Inhibitors + TGF-β1-Cy3. (E) Representative western blot showing the kinase inhibitor combination does not prevent TGF-β1 increases in phospho-cofilin1 levels as confirmed by analysis of data presented as mean ± SEM. (A, B, E) n=5. (C, D) n=3. Two-way ANOVA is used for (A, C, E). two-tailed paired Student's t test applied for (B, D). *p<0.05, **p<0.01, ***p<0.001. ns, not significant.
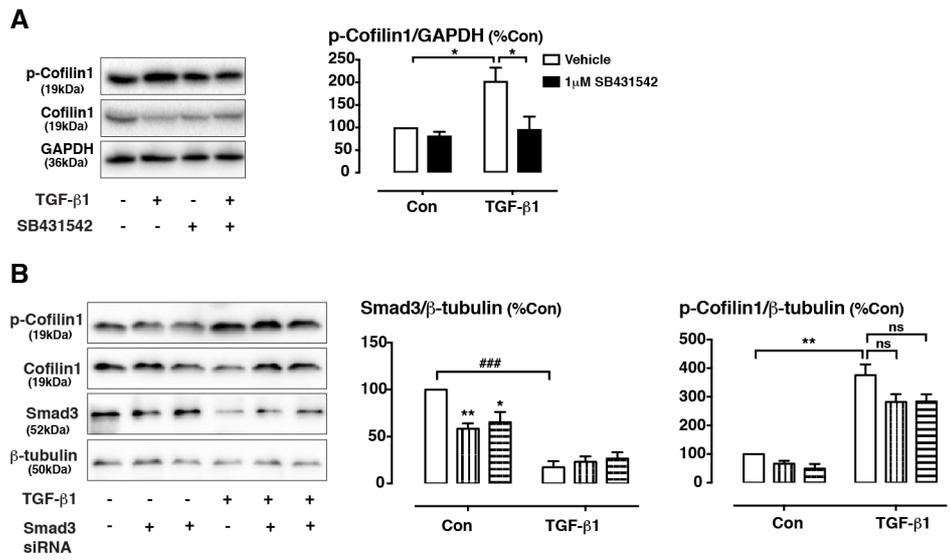
Figure S2. TGF-β1-induced phospho-cofilin1 is dependent on ALK5, but not Smad3 activity, related to Figure 2. (A) BEAS-2B cells were pre-incubated with SB431542 (1μM) for 30min prior to incubation with TGF-β1 (40pM) for 24h. **(B)** BEAS-2B cells transiently transfected with Smad3-targeted siRNA were incubated with TGF-β1 (40pM) for 24h. The representative blot and quantification are shown here. Results are presented as mean ± SEM for n=3-4. Two-way ANOVA and two-tailed paired Student's t test are used. *p<0.05, **p<0.01, ###p<0.001.
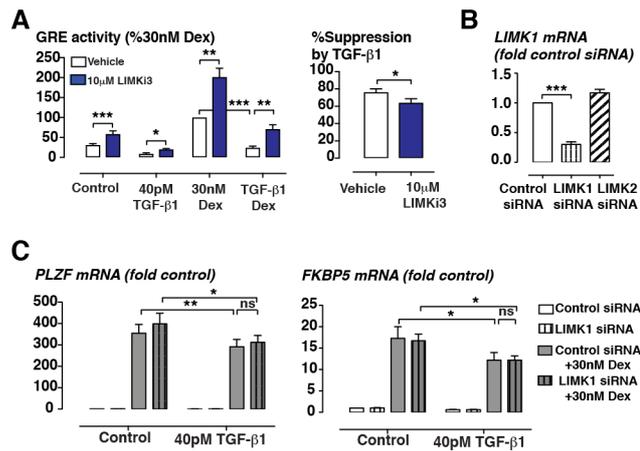
Figure S3. Pharmacological inhibition of LIMK attenuates TGF-β1 suppression of GRE activity, related to Figure 3. (A, B) BEAS-2B cells transiently transfected with GRE-SEAP reporter constructs were incubated with LIMKi3 (10μM) 30min prior to TGF-β1 (40pM) for 24h, then stimulated with Dex (30nM) for another 24h. (C) BEAS-2B cells transfected with negative control, LIMK1-targeted siRNA, were incubated with TGF-β1 (40pM) for 24h, followed by incubation with Dex (30nM) for 4h for mRNA measurement. Results are presented as mean ± SEM. (A, B, C) n=5. Two-way ANOVA is used for (A, C); two-tailed Student's t test is used for (A, B). *p<0.05, **p<0.01, ***p<0.001.
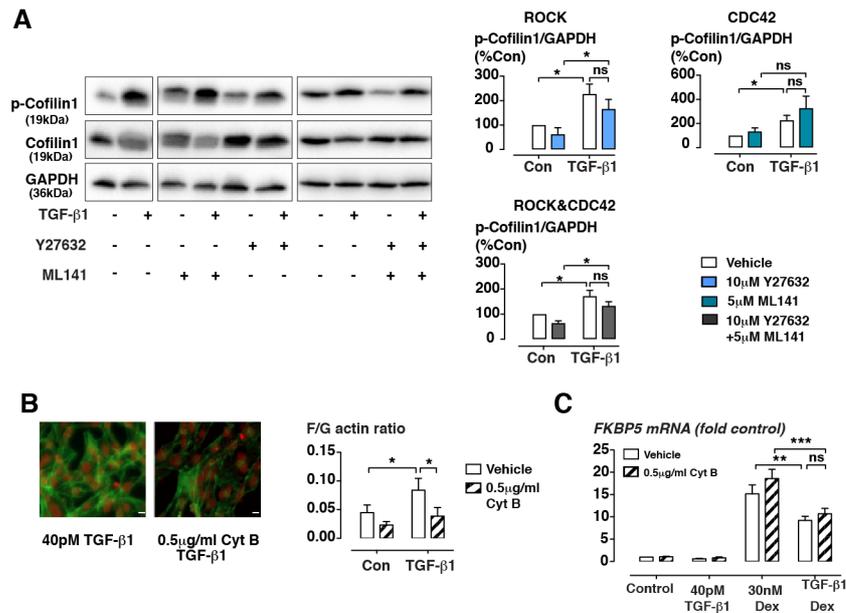
Figure S4. Pharmacological inhibition of ROCK/Cdc42 does not prevent TGF-β1-induced phospho-cofilin1; TGF-β1-induced actin reorganization does not affect TGF-β1 repression of GC target gene expression, related to Figure 4. (A) Serum-starved BEAS-2B cells were pre-incubated with either ROCK inhibitor (Y27632, 10μM), or Cdc42 inhibitor (ML141, 5μM), or combined inhibitors (10μM Y27632 and 5μM ML141), 30 minutes prior to TGF-β1 (40pM) for 24 hours. Cell lysate were collected and subjected to western blotting. Result is presented as mean ± SEM for n=4 independent experiments. (B, C) F-G actin staining for BEAS-2B cells incubated cytochalasin B (0.5μg/ml) with 30min prior to TGF-β1 (40pM) for 24h. scale bar=50μm. Effects of cytochalasin B (0.5μg/ml) on TGF-β1 impairment of GC-inducible gene expression. Two-way ANOVA is used. *p<0.05, **p<0.01, ***p<0.001.
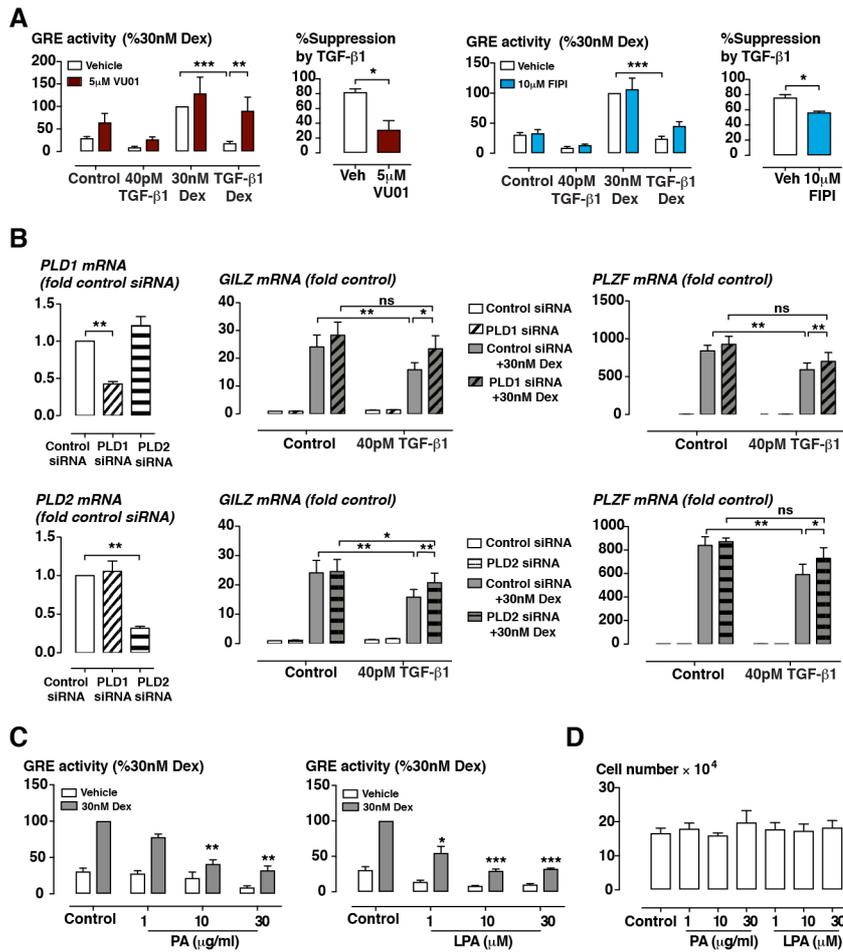
Figure S5. Inhibition of PLD attenuates TGF-β1 suppression of GC activity, and exogenous PLD products mimic TGF-β1 effects, related to Figure 5. (A) BEAS-2B cells transiently transfected with GRE-SEAP reporter constructs were incubated with either VU0155069 (5μM) or FIPI (10μM) 30min prior to TGF-β1 (40pM) for 24h, then incubated with Dex (30nM) for another 24h for GRE-SEAP measurement. (B) Effects of individual PLD1 or PLD2 siRNA on PLD1 and PLD2 mRNA expression, respectively, and on TGF-β1 suppression of Dex-inducible gene expression in BEAS-2B cells. (C) BEAS-2B cells transiently transfected with GRE-SEAP reporter constructs were incubated with either PA (1-30μg/ml) or LPA (1-30μM) 30min prior incubation with Dex (30nM) for another 24h for GRE-SEAP measurement. (D) Experiments of the same duration as in (C) were undertaken to ascertain the cytotoxicity, if any, of PA or LPA by measuring viable cell numbers at the end of the incubation period. Data are presented as mean ± SEM. (A-D) n=4-5. Two-way ANOVA and two-tailed Student's t test are used. *p<0.05, **p<0.01, ***p<0.001.
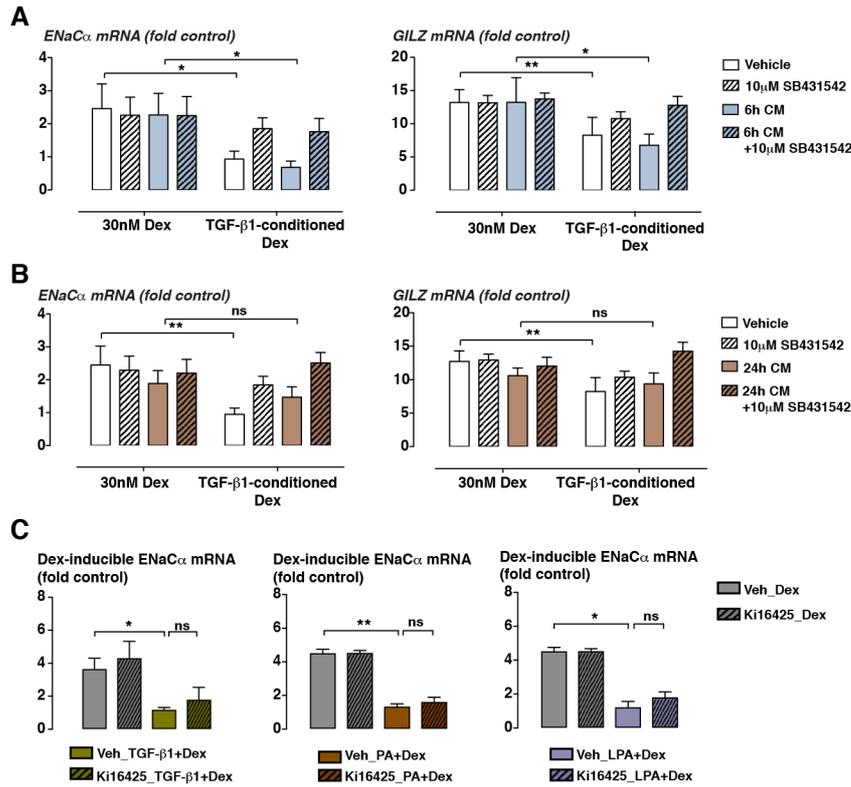
Figure S6. TGF-β1 suppression of GC activity is not due to an extracellular product, related to figure 5. (A, B) BEAS-2B cell were incubated with vehicle or TGF-β1 (40pM) for 6h (A) or 24h (B) to generate conditioned medium. Vehicle or SB431542 (10μM) was added to conditioned medium prior to its addition to serum-starved BEAS-2B cells. Cells were incubated directly with TGF-β1 (40pM) or pre-treated with conditioned medium for another 24h, then incubated with Dex (30nM) for 4h before mRNA measurement. (C) Blockade of LPA receptor does not influence the impairment of GC inducible gene expression. BEAS-2B cells were incubated with Ki16425 (10μM) 30min prior to TGF-β1 (40pM), or PA (30μg/ml), or LPA (30μM) for 24h, prior to the stimulation with Dex (30nM) for 4h. Data are presented as mean ± SEM. (A) n=4, (B) n=5, (C) 3-4. CM, conditioned medium. Two-way ANOVA is used for (A, B, C). ns, not significant. *p<0.05, **p<0.01.
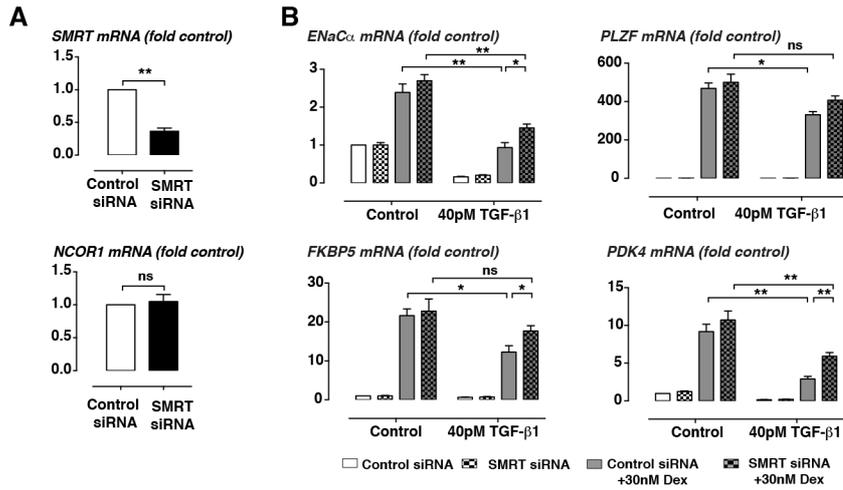
Figure S7. Genetic deletion of SMRT attenuates TGF-β1-induced repression of GR target genes, related to figure 6. (A, B) BEAS-2B cells transfected with negative control siRNA, SMRT-targeted siRNA, were incubated with TGF-β1 (40pM) for 24h, then incubated with Dex (30nM) for another 4h before mRNA measurement. Data are presented as mean±SEM. (A, B) n=4. ns, not significant. Two-way ANOVA and two-tailed Student's t test are used. *p<0.05, **p<0.01.
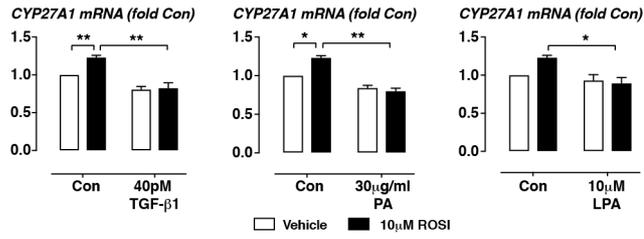
Figure S8. PPARγ-targeted gene is inhibited by TGF-β1, PA and LPA, related to figure 6. Serum starved BEAS-2B cells were treated with either TGF-β1 (40pM), or PA (30μg/ml), or LPA (30μM) for 24h, and then stimulated with rosiglitazone (ROSI, 10μM) for a further 4h, after which RNA was extracted and analysed by qRT-PCR. Results are presented as mean ± SEM. n=4. Two-way ANOVA is used. *p<0.05, **p<0.01.

Table S2. Classification of specific TGF-β1-impaired Dex-responsive genes based on the distribution of pGRE and nGRE, related to Figure 1.

			nGRE	pGRE	Both	None	Total
Dex up-regulated genes	**Unimpaired**	TGF-β1+Dex>Dex	**0**	**35**	**3**	**53**	91
	impaired	TGF-β1+Dex<Dex	**11**	**75**	**7**	**120**	213
Dex down-regulated genes	**Unimpaired**	TGF-β1+Dex<Dex	**1**	**12**	**0**	**27**	40
	impaired	TGF-β1+Dex>Dex	**9**	**55**	**5**	**112**	181

Fisher's exact test comparing the number of Dex up-regulated genes impaired by TGF-β1 (TGF-β1+Dex<Dex), comparing those genes bearing an nGRE and those bearing a pGRE in the promoter, p=0.03

Table S4. List of differentially expressed proteins identified by mass spectrometry, related to Figure 2.

	Master#	Protein ID	t-test	Ave Ratio	Protein Score	PI
1	361	Tropomyosin 1 (Alpha) isoform 1	0.037	2.01	787	4.69
2	478	Phosphoglycerate mutase 1	0.070	1.89	148	6.67
3	525	Triosephosphate isomerase	0.050	1.44	931	6.45
4	537	Proteasome subunit alpha type	0.049	-1.42	184	8.59
5	715	Cofilin-1 (p)	0.014	1.78	435	8.51

Table S5. Demographic data for subjects from the MESCA cohort from whom biopsies were obtained for immunohistochemistry, related to Figure 2.

	Non-Asthma	Mild Asthma[#]	Moderate Asthma[#]	Severe Asthma[#]
Subject n (M/F)	10 (6/4)	10 (6/4)	7 (7/0)	9 (2/7)
FEV_1 % predict	108 (98-115)	103 (94-107)	60 (57-65)	64 (58-80)
Atopic (%)	50	90	100	56
Current smokers (%)	50	30	14	0
Current treatment (%)				
β_2-adrenoceptor agonists	0	90	100	100
Inhaled steroids	0	80	100	100
Oral steroids	0	20	14	100

Data presented as median (interquartile range) or %. M: male; F: female; FEV_1: forced expiratory volume in one second; % pred: % predicted. [#]: classified using Global Initiative for Asthma guidelines.

Transparent Methods

Cell culture and reagents. BEAS-2B bronchial and A549 lung adenocarcinoma epithelial cells were cultured as described previously (Salem et al., 2012). Primary HBECs were purchased from Lonza and cultured using B-ALI[TM] BulletKit[TM] (Lonza) according to manufacturer's instructions. Primary HBECs were seeded and differentiated for 28 days at air-liquid interface on fibrillar collagen (30μg/ml)-coated 24-well Corning® Transwell® inserts (0.4μm) (Sigma-Aldrich, CLS3470-48EA). Cell differentiation was confirmed by the measurement of trans-epithelial electrical resistance (TEER) using an EVOM2 Voltammeter (WPI, Sarasota, FL) and visualization of beating cilia.

Main reagents used in this study are as follow: Recombinant human TGF-β1 protein (R&D systems, 240-B-002); Recombinant human TGF-β2 protein (Sino Biological Inc., 10382-H08H); Recombinant human TGF-β3 protein (PeproTech, AF-100-36E); Dexamethasone (Sigma-Aldrich, D1756); SB202190 (CalBiochem, 559388); U0126 (Merck Millipore, 662005); SP600125 (Merck Millipore, 420119); LY294002 (Merck Millipore, 440202); LIMKi3 (Merck Millipore, 435930); Y27632 (TOCRIS, 1254); ML141 (TOCRIS, 4266); Cytochalasin B (Sigma-Aldrich, C6762); VU0155069 (Santa Cruz Biotechnology, sc-224371A); FIPI (Santa Cruz Biotechnology, sc-294594); PA (Sigma, P9511); LPA (Sigma, L7260); SB431542 (Sigma, S4317); Ki16425 (Cayman, 10012659).

Transcriptomic analysis. Biological replicates (n=3) of samples underwent RNA-seq was performed in the Melbourne Translational Genomic Platform, University of Melbourne. All clean reads were mapped to the human reference genome GRCh38-hg38 assembly using Rsubread package. Read alignment was conducted using featureCount and gene expression values were calculated for each gene as counts per million (cpm). Relative transcript abundances and differentially expressed genes were then determined using the edgeR package. Genes with less than 1 cpm in at least three samples were filtered out from further analyses, the remaining gene expression levels were then subjected to pairwise comparisons to identify differentially expressed genes applying a "Benjamini and Hochberg" multiple comparison correction and applying a significance threshold of FDR<0.05. In order to analyze the use of the different GRE elements we annotated our genes using annotations derived from the literature (Surjit et al., 2011) and gene lists derived from EnrichR website (generated from encode and Transfac annotation). We analysed the relative enrichment in GRE among those genes differentially expressed by Dex and Dex in the presence of TGF-β1 using a Fisher's exact test. FunRich (v3.1.3), an open access standalone tool, was used to perform functional enrichment analysis.

Data and Software Availability. All sequencing data are available from GEO under series number GSE104908

Two-dimensional differential in gel electrophoresis (2D-DIGE). 2D-DIGE experiments were performed by using the minimal fluorescent labeling. Firstly, BEAS-2B cell lysates were harvested in solubilisation solution (7M urea, 2M thiourea, 4% CHAPS, 30mM Tris-HCl, pH8.5) containing phosphatase inhibitor cocktail (Sigma-Aldrich, P5726) and protease inhibitor cocktail (Sigma-Aldrich, P1860). Protein concentration was measured with Bradford protein assay (Bio-Rad, 500-0006). Secondly, minimal fluorescent labeling was conducted at a ratio of 400pmol CyDye (Cy3/Cy5, Lumiprobe) per 50μg protein. Simultaneously, an internal pooled standard consisting of equal aliquots from samples under comparison was labeled with Cy2. For each set of experiments, three or five gels were run for statistical analysis (t-test), and Cy3/Cy5 reverse labeling was performed to minimize potential dye labeling variability. Subsequently, the Immobiline DryStrips (7cm, pH3-10, BioRad) were rehydrated overnight with the combined labeled samples via passive loading. The isoelectric focusing was performed in an IPGphor Isoelectric focusing system (BioRad) according to the following schedule: (1) linear increase from 0 to 250V in 20min; (2) rapid increase from 250V to 4000V within 2h; (3) hold 4000V for 3h. Strips were then submitted directly to the second-dimension electrophoresis. SDS-PAGE was performed using XCell SureLock Mini-Cell Electrophoresis System. IPG strips were denatured and reduced in the equilibration buffer (6M urea, 2% (w/v) SDS, 30% (v/v) glycerol, 50mM Tris-HCl, 65mM DTT, pH 8.8) for 15min, then alkylated in equilibration buffer with 135mM iodoacetamide for 15min. The IPG strips were loaded onto a Ready Gel® IEF Precast Gels, which were run at the constant electromagnetic force 200V for approximately 40 minutes. Gels were scanned using the Typhoon-Variable mode imager (GE healthcare) with 487, 532 and 635nm lasers for Cy2, Cy3 and Cy5, respectively. Image analysis was performed using DeCyder V7.0 software. Comparisons between all gels were conducted using an paired Student's t-test analysis, which determined the variation between

different treatments. Differential expressions of proteins present in the gels were deemed significant by a fold change of ≥ 1.2 and a p-value of <0.05.

Protein spots that displayed statistically significant differential expression were selected for identification by LC-MS/MS (liquid chromatography-tandem mass spectrometry). Fifty micro grams of TGF-β1-treated sample was taken from each of the biological replicates in the experimental series and pooled to form a preparative gel sample. The preparative gel was used for spot picking and later for protein identification by MS/MS. The preparative gel was then stained with Coomassie Blue G-250 for visualizing pick-up. A pick list containing the specific locations of proteins of interest on the gel was generated. The gel plugs consisting of the proteins of interest were manually excised from the preparative gel, then digested with modified porcine trypsin protease (Sigma-Aldrich, T6567) following the described protocol (Shevchenko et al., 2006). Samples were subjected to LC-MS/MS with an OrbiTRAP ELITE ETD mass spectrometer (Thermo Scientific). Briefly, 2μl containing tryptic peptides was applied to a C18 reversed-phase HPLC column (Dionex, 15cmx75μm) using a nanoUPLC system (Dionex, Ultimate 3000 RSLC). Bound peptides were eluted with a gradient mixture of solvent A (0.1% v/v formic acid) and solvent B (100% acetonitrile in 0.1% formic acid (v/v)) as follows: 3–12% B 1 min; 12–35% B 20 min; 35–80% B 2 min. Eluted peptides were analysed in Fourier transform mode (240,000 resolution) with mass range 300–1650 m/z, and the 20 most-intense peptide ions were automatically selected for MS/MS using collision-induced fragmentation in the linear ion trap. Peak lists were searched against the Uniprot human database using MASCOT (fixed modification: carbamidomethly Cys; variable modifications: oxidized Met, phosphorylated Ser/Thr/Tyr). Protein identifications were assigned on the basis of significance (p < 0.01), concordance of observed and theoretical mass and p*I* from 2D gel positions, and with the requirement that at least two peptides were confidently assigned.

Cell transfection. BEAS-2B cells were seeded at the density of 75,000 cells/well in 24-well plate in penicillin-streptomycin free medium overnight. Cells were co-transfected with pGRE-SEAP (Clontech Laboratories Inc., Mountain View, CA) and pGL3-Luc (Promega, Alexandria, NSW, Aus) plasmids using Lipofectamine® 2000 (Invitrogen, Carlsbad, CA). Transfected cells were pretreated with inhibitors 30min prior to 40pM TGF-β1 for 24h or directly treated with TGF-β isoforms, and then incubated with 30nM Dex for another 24h. Supernatants were collected for measurement of secreted human placental alkaline phosphatase (SEAP) following the instructions for chemiluminescence kit (Roche Applied Science, NSW, Aus). Luciferase expression was determined as transfection efficiency control as described. Pre-validated siRNAs (sequences shown as below) were transfected using Lipofectamine RNAiMAX (Invitrogen). 24h after transfection, cells were treated with 40pM TGF-β1 for 24h, and then incubated with 30nM Dex for further 4h after which total RNA was extracted to assess GC activity.

Target	siRNA ID	Sequences
CFL1 (Cofilin1)	s2937	UUCAUGUCGUUGAACACCUTG
CFL1 (Cofilin1)	s2938	UGCAAUUCAUGCUUGAUCCCT
LIMK1	s8188	UGUAUCGUGAGGGUCAUGCTC
LIMK2	s8192	UCAAUGAUCACCUUGCAGCTC
LIMK2	s8193	AAUGAUCUCACAGAGAACGAT
SMAD3	s8401	UAGGGAUUCACGCAGACCUCG
SMAD3	s8402	UUCGGGUCAACUGGUAGACAG
PLD1	s10638	UUUCGAUAUAGAUAUAGUGCC
PLD2	s10640	UUGCGAUAGAAAGACAUGGTC
NCOR2 (SMRT)	s18468	UCAGCUUAGAGAUCUGCUGCT
NCOR2 (SMRT)	s18469	UUGUUUCCGAGCGUGAUUCCT

Western Blot Analysis. Western blotting was performed as described (Khau et al., 2011). Rabbit monoclonal anti-FKBP5 [EPR6617] (Abcam, ab126715) and mouse monoclonal anti-PLZF (D-9) (Santa cruz, sc-28319) were used to determine TGF-β1 impact on Dex-inducible proteins. Rabbit monoclonal anti-phospho-cofilin1 (Ser3) (Cell signaling, 3313) and mouse monoclonal anti-cofilin1 (Abcam, ab54532) were used to assess TGF-β1 induction on phospho-cofilin1. Rabbit monoclonal anti-SMRT (Cell signaling, 62370) and rabbit monoclonal anti-Smad3 (Cell signaling, 9523) were used to assess SMRT and Smad3 level change. Anti-GAPDH (Abcam, ab37168) and anti-β-tubulin (Merck Millipore,

MAB3408) were used as housekeeping proteins for loading control. Densitometry was performed using the image J program (1.48v, National Institute of Health, USA).

RNA extraction and Quantitative Real Time PCR (qRT-PCR). Total RNA was extracted and real-time PCR assays were performed using SYBR green reagents (BioRad). Primer sequences are listed as below.

Genes	Primer sequences (5' to 3')
18srRNA[#]	FP: CGCCGCTAGAGGTGAAATTC
	RP: TTGGCAAATGCTTTCGCTC
GILZ[#]	FP: TCCTGTCTGAGCCCTGAAGAG
	RP: AGCCACTTACACCGCAGAAC
ENaCα[#]	FP: AGCACAACCGCATGAAGAC
	RP: TGAGGTTGATGTTGAGGCTG
PDK4[#]	FP: CTTGGGAAAAGAAGACCTTAC
	RP: GTGCAGTGGAGTATGTATAAC
PLZF[#]	FP: GTTCCTGGATAGTTTGCG
	RP: CATGTCAGTGCCAGTATG
PAI-1[#]	FP: TCAGGCTGACTTCACGAGTCTTT
	RP: CTGCGCGACGTGGAGAG
FKBP5[#]	FP: AGATTGAGCTCCTTGATTTC
	RP: TGAATATCCCTCTCCTTTCC
CDKN1C[#]	FP: TCTGATCTCCGATTTCTTCG
	RP: CTCTTTGGGCTCTAAATTGG
CFL-1*	FP: CTATGATGCAACCTATGAGAC
	RP: CTGTCAGCTTCTTCTTGATG
LIMK1*	FP: GCTATCAAGGTGACACAC
	RP: ATGTACTCAGTGATGAAGTTG
LIMK2*	FP: CTTTCACCTCAGTCAGAAAAG
	RP: TATCAAGGTGACACACAAAG
PLD1*	FP: AAAAGATCTGGAGGACACAG
	RP: CCATCTTTTTGACCATCTGTAG
PLD2*	FP: AAGACTCATCCTCTAGGAAC
	RP: ATCTATGAGCAGATCTTCCG
CYP27A1*	FP: ATACGGATGCTTTCAATGAG
	RP: CGAACAGGATGTAGCAAATAG

\# Primer sequences were obtained from the literature (Keenan et al., 2014; Salem et al., 2012)
* KiCqStart pre-designed primers were purchased from Sigma-Aldrich

Immunohistochemistry (IHC). Subjects used in this study were either nonasthmatic or asthmatics with varying asthma severities (classified by using Global initiative for Asthma guidelines) recruited from the Melbourne Epidemiological Study of Childhood Asthma (MESCA) cohort (all aged 42 years at the time of biopsy). The demographic data are provided in Table S5.
Paraffin embedded sections of human airway (3μm) were stained with rabbit monoclonal antibodies to phospho-cofilin1 (Cell signaling, 3313), or IgG isotype control (Cell signaling, 3900) following the three layer immunoperoxidase staining protocol. Antibody staining was completed using the Dako EnVision anti-rabbit kit as appropriate (Dako, Carpinteria, CA), where sections were counterstained with hematoxylin. More detailed studies on the MESCA (Melbourne Epidemiological Study of Childhood Asthma) cohort used in this study (Phelan et al., 2002) (Tai et al., 2014) and other IHC studies have been reported (Qiao et al., 2017; Ward et al., 2008).

Staining for F-G actin. BEAS-2B cells were seeded onto 8-well chamber slides overnight, and then maintained in serum-free medium for 24h. After that, cells were pretreated with different inhibitors 30min prior to 40pM TGF-β1 for further 24h. For F- and G-actin staining, cells were fixed in 10% (v/v) neutral buffered formalin (NBF) for 15min and permeabilized with 0.2% (v/v) Triton X-100 for 5min. After washing in PBS, cells were blocked with 0.1% Triton X-100 in 1% BSA/PBS solution for 15min, and then stained with Oregon-green 488 (green) phalloidin (1:50, Invitrogen Molecular Probes, O7466) and Alex-Fluor 594 (red) deoxyribonuclease1 (DNase1)-texas red conjugate (10mg/ml, Invitrogen

Molecular Probes, D12372) for 20min at room temperature. Under these conditions, phalloidin and DNase1 bind F- and G-actin, respectively. Nuclei were stained with 4',6-diamidno-2-pheylindole (DAPI) (1:100 in PBS) for 10 min. Slides were mounted using DAKO fluorescent mounting media and examined using a Zeiss fluorescence microscope-live cell imaging system.

Quantification of cytokines in supernatants by Enzyme-linked Immunosorbent Assay (ELISA). Supernatant were collected for measurement of cytokines like IL-8 (BD optEIA™, 555126), granulocyte macrophage colony-stimulating factor ((GM-CSF), BD optEIA™, 555244) by ELISA following the manufacturers' instructions.

Cell Viability. Cell viability was assessed using the Trypan blue exclusion method. Briefly, cells were initially inspected under the microscope for the presence of detached cells. Cell monolayers were then washed with 1mL PBS, and then harvested by the addition of trypsin prior to incubation with Trypan blue (0.25% (w/v) in 2% fetal bovine serum) for 5 minutes before counting stained and unstained cells.

Statistical analyses. Data are presented as the mean ± SEM for n individual experiments. All data were statistically analyzed using GraphPad Prism 5.0 for Mac (Graphpad Software, San Diego, CA). One-way or two-way analyses of variance (ANOVA) with Bonferroni's *post hoc* test were used to analyze the data. In some cases, paire two-tailed Student's t test is used. A P value less than 0.05 was considered to be statistically significant.

Supplemental References

Keenan, C.R., Mok, J.S., Harris, T., Xia, Y., Salem, S., and Stewart, A.G. (2014). Bronchial epithelial cells are rendered insensitive to glucocorticoid transactivation by transforming growth factor-beta1. Respiratory research *15*, 55.

Khau, T., Langenbach, S.Y., Schuliga, M., Harris, T., Johnstone, C.N., Anderson, R.L., and Stewart, A.G. (2011). Annexin-1 signals mitogen-stimulated breast tumor cell proliferation by activation of the formyl peptide receptors (FPRs) 1 and 2. FASEB J *25*, 483-496.

Phelan, P.D., Robertson, C.F., and Olinsky, A. (2002). The Melbourne Asthma Study: 1964-1999. J Allergy Clin Immunol *109*, 189-194.

Qiao, Y., Tam, J.K.C., Tan, S.S.L., Tai, Y.K., Chin, C.Y., Stewart, A.G., Ashman, L., Sekiguchi, K., Langenbach, S.Y., Stelmack, G., *et al*. (2017). CD151, a laminin receptor showing increased expression in asthmatic patients, contributes to airway hyperresponsiveness through calcium signaling. J Allergy Clin Immunol *139*, 82-92 e85.

Salem, S., Harris, T., Mok, J.S., Li, M.Y., Keenan, C.R., Schuliga, M.J., and Stewart, A.G. (2012). Transforming growth factor-beta impairs glucocorticoid activity in the A549 lung adenocarcinoma cell line. British journal of pharmacology *166*, 2036-2048.

Shevchenko, A., Tomas, H., Havlis, J., Olsen, J.V., and Mann, M. (2006). In-gel digestion for mass spectrometric characterization of proteins and proteomes. Nat Protoc *1*, 2856-2860.

Surjit, M., Ganti, K.P., Mukherji, A., Ye, T., Hua, G., Metzger, D., Li, M., and Chambon, P. (2011). Widespread negative response elements mediate direct repression by agonist-liganded glucocorticoid receptor. Cell *145*, 224-241.

Tai, A., Tran, H., Roberts, M., Clarke, N., Gibson, A.M., Vidmar, S., Wilson, J., and Robertson, C.F. (2014). Outcomes of childhood asthma to the age of 50 years. J Allergy Clin Immunol *133*, 1572-1578 e1573.

Ward, J.E., Harris, T., Bamford, T., Mast, A., Pain, M.C., Robertson, C., Smallwood, D., Tran, T., Wilson, J., and Stewart, A.G. (2008). Proliferation is not increased in airway myofibroblasts isolated from asthmatics. Eur Respir J *32*, 362-371.